

4509  
12-17-84 JS (3)

I-18534

DR-0670-X

# SANDIA REPORT

SAND84-1589 • Unlimited Release • UC-66c

November 1984

SAND--84-1589

DE85 004356

## Computer Simulation of the Cooling Effect Due to Circulation in Four Geothermal Well Models

**NOTICE**  
**PORTIONS OF THIS REPORT ARE ILLEGIBLE.**

It has been reproduced from the best available copy to permit the broadest possible availability.

Leonard E. Duda

Prepared by  
Sandia National Laboratories  
Albuquerque, New Mexico 87185 and Livermore, California 94550  
for the United States Department of Energy  
under Contract DE-AC04-76DP00789



## **DISCLAIMER**

**This report was prepared as an account of work sponsored by an agency of the United States Government. Neither the United States Government nor any agency Thereof, nor any of their employees, makes any warranty, express or implied, or assumes any legal liability or responsibility for the accuracy, completeness, or usefulness of any information, apparatus, product, or process disclosed, or represents that its use would not infringe privately owned rights. Reference herein to any specific commercial product, process, or service by trade name, trademark, manufacturer, or otherwise does not necessarily constitute or imply its endorsement, recommendation, or favoring by the United States Government or any agency thereof. The views and opinions of authors expressed herein do not necessarily state or reflect those of the United States Government or any agency thereof.**

## **DISCLAIMER**

**Portions of this document may be illegible in electronic image products. Images are produced from the best available original document.**

Issued by Sandia National Laboratories, operated for the United States Department of Energy by Sandia Corporation.

**NOTICE:** This report was prepared as an account of work sponsored by an agency of the United States Government. Neither the United States Government nor any agency thereof, nor any of their employees, nor any of their contractors, subcontractors, or their employees, makes any warranty, express or implied, or assumes any legal liability or responsibility for the accuracy, completeness, or usefulness of any information, apparatus, product, or process disclosed, or represents that its use would not infringe privately owned rights. Reference herein to any specific commercial product, process, or service by trade name, trademark, manufacturer, or otherwise, does not necessarily constitute or imply its endorsement, recommendation, or favoring by the United States Government, any agency thereof or any of their contractors or subcontractors. The views and opinions expressed herein do not necessarily state or reflect those of the United States Government, any agency thereof or any of their contractors or subcontractors.

Printed in the United States of America  
Available from  
National Technical Information Service  
U.S. Department of Commerce  
5285 Port Royal Road  
Springfield, VA 22161

NTIS price codes  
Printed copy: A04  
Microfiche copy: A01

SAND84-1589

COMPUTER SIMULATION OF THE COOLING EFFECT  
DUE TO CIRCULATION IN FOUR GEOTHERMAL WELL MODELS

Leonard E. Duda

---

**DISCLAIMER**

This report was prepared as an account of work sponsored by an agency of the United States Government. Neither the United States Government nor any agency thereof, nor any of their employees, makes any warranty, express or implied, or assumes any legal liability or responsibility for the accuracy, completeness, or usefulness of any information, apparatus, product, or process disclosed, or represents that its use would not infringe privately owned rights. Reference herein to any specific commercial product, process, or service by trade name, trademark, manufacturer, or otherwise does not necessarily constitute or imply its endorsement, recommendation, or favoring by the United States Government or any agency thereof. The views and opinions of authors expressed herein do not necessarily state or reflect those of the United States Government or any agency thereof.

**MASTER**

*eb*  
DISTRIBUTION OF THIS DOCUMENT IS UNLIMITED

## ABSTRACT

Computer calculations of wellbore transient temperatures, using the geothermal wellbore thermal simulator code GEOTEMP2, were made on four well models. The well models studied were from the Baca geothermal area, the East Mesa geothermal area, and a shallow and a deep well from the Salton Sea geothermal area. Calculations for one day of water circulation followed by one day of shut-in at flow rates of 100, 250, 500, and 1000 gpm were made to investigate the cooling effects produced by the circulation. Additional calculations were made using the Baca and Salton Sea well models. In the former, the effect on the cooling due to different soil thermal conductivity values and different circulating fluids (a high viscosity mud and air) were investigated. In the latter, the number of casings in the wellbore and the diameter of the tubing were modified. Plots of the calculated temperatures as a function of circulation and shut-in time and depth are given for each case.

Some conclusions which may be drawn are:

- o Low flow rates, on the order of 100 gpm or less, are particularly ineffective at cooling the wellbore.
- o Low soil thermal conductivity values produce lower wellbore temperatures.
- o High viscosity fluids, such as drilling muds, give lower wellbore temperatures.
- o Air or gas are ineffective as a cooling fluid.
- o For a purely conductive environment (i.e. no fluid convection into the rock formation), temperatures tend to recover quickly following circulation. Mean temperatures are reached 3-5 hours following shut-in.
- o Downhole temperatures are not directly proportional to circulation time.
- o The shape of the undisturbed temperature profile has a significant effect upon the downhole temperatures.
- o An increased fluid velocity in the tubing tends to decrease the downhole temperatures in the wellbore.

## TABLE OF CONTENTS

|   | Page |
|---|------|
| 1. INTRODUCTION . . . . .                             | 1    |
| 2. WELL MODEL CALCULATIONS . . . . .                  | 1    |
| 2.1 GEOTEMP2 COMPUTER CODE . . . . .                  | 3    |
| 3. WELL MODEL RESULTS . . . . .                       | 5    |
| 3.1 BACA WELL MODEL . . . . .                         | 5    |
| 3.1.1 STANDARD WELLBORE CALCULATIONS AND RESULTS. . . | 5    |
| 3.1.2 PARAMETRIC STUDY OF THE BACA WELL MODEL. . .    | 14   |
| 20 DAY CIRCULATION TIME . . . . .                     | 14   |
| MUD AS THE CIRCULATING FLUID . . . . .                | 21   |
| AIR AS THE CIRCULATING FLUID . . . . .                | 26   |
| 3.2 SALTON SEA WELL MODEL . . . . .                   | 28   |
| 3.2.1 STANDARD WELLBORE CALCULATIONS AND RESULTS .    | 28   |
| 3.2.2 MODIFIED WELLBORE CALCULATIONS AND RESULTS .    | 33   |
| THREE CASING STRINGS . . . . .                        | 33   |
| REDUCED TUBING DIAMETER . . . . .                     | 37   |
| 3.3 EAST MESA WELL MODEL . . . . .                    | 41   |
| 3.3.1 STANDARD WELLBORE CALCULATIONS AND RESULTS. .   | 41   |
| 3.4 DEEP SALTON SEA WELL MODEL . . . . .              | 46   |
| 3.4.1 STANDARD WELLBORE CALCULATIONS AND RESULTS .    | 46   |
| 4. SUMMARY AND CONCLUSIONS . . . . .                  | 51   |
| REFERENCES . . . . .                                  | 54   |

## LIST OF FIGURES

| Figure   | Page |
|--|------|
| 3-1 The wellbore geometry and undisturbed temperature gradient used in the Baca well model calculations . . .  | 6    |
| 3-2 Bottom-hole temperatures as a function of time during circulation and following shut-in at four flow rates and three soil conductivities for the Baca well model . . . . .   | 7    |
| 3-3 The downhole temperature profiles at times of 0, 2, 5, 10, 12, 16, and 24 hours following shut-in at four flow rates and a soil thermal conductivity of 0.5 Btu/ft hr <sup>OF</sup> for the Baca well model . . . . .  | 8    |
| 3-4 The downhole temperature profiles at times of 0, 2, 5, 10, 12, 16, and 24 hours following shut-in at four flow rates and a soil thermal conductivity of 1.0 Btu/ft hr <sup>OF</sup> for the Baca well model . . . . .  | 9    |
| 3-5 The downhole temperature profiles at times of 0, 2, 5, 10, 12, 16, and 24 hours following shut-in at four flow rates and a soil thermal conductivity of 2.0 Btu/ft hr <sup>OF</sup> for the Baca well model . . . . .  | 10   |
| 3-6 The return temperatures at the surface in the annulus at four flow rates and three soil thermal conductivities for the Baca well model. . . . .  | 13   |
| 3-7 Comparison of the bottom-hole temperatures following shut-in for circulation times of 1 and 20 days at flow rates of 250 and 1000 gpm and soil thermal conductivities of 0.5 and 2.0 Btu/ft hr <sup>OF</sup> . . .   | 15   |
| 3-8 Comparison of the downhole temperatures at times of 0, 2, 5, 10, 12, 16, and 24 hours following shut-in at circulation times of 1 and 20 days for flow rates of 250 and 1000 gpm and a soil thermal conductivity of 0.5 Btu/ft hr <sup>OF</sup> for the Baca well model. . . . .                                 | 16   |
| 3-9 Comparison of the downhole temperatures at times of 0, 2, 5, 10, 12, 16, and 24 hours following shut-in at circulation times of 1 and 20 days for flow rates of 250 and 1000 gpm and a soil thermal conductivity of 2.0 Btu/ft hr <sup>OF</sup> for the Baca well model. . . . .                                 | 17   |
| 3-10 Comparison of the radial temperature profiles for circulation times of 1 and 20 days at flow rates of 250 and 1000 gpm and a soil thermal conductivity of 0.5 Btu/ft hr <sup>OF</sup> . Temperatures are plotted at depths of 610 m (2000 ft), 914 m (3000 ft), 1220 m (4000 ft), and 1830 m (6000 ft). . . . . | 19   |

## LIST OF FIGURES

| Figure |   | Page |
|--------|---|------|
| 3-11   | Comparison of the radial temperature profiles for circulation times of 1 and 20 days at flow rates of 250 and 1000 gpm and a soil thermal conductivity of 2.0 Btu/ft hr <sup>OF</sup> . Temperatures are plotted at depths of 610 m (2000 ft), 914 m (3000 ft), 1220 m (4000 ft), and 1830 m (6000 ft). . . . . | 20   |
| 3-12   | Bottom-hole temperatures as a function of time during circulation and following shut-in at four flow rates and three soil conductivities for the Baca well model using mud as the circulating fluid..   | 22   |
| 3-13   | The downhole temperature profiles at times of 0, 2, 5, 10, 12, 16, and 24 hours following shut-in at four flow rates and a soil thermal conductivity of 1.0 Btu/ft hr <sup>OF</sup> for the Baca well model using mud as the circulating fluid. . . . .   | 23   |
| 3-14   | Comparison of the radial temperature profiles for circulation with water or mud . . . . .   | 24   |
| 3-15   | The return temperatures at the surface in the annulus at four flow rates and three soil thermal conductivities for the Baca well model using mud as the circulating fluid. . . . .  | 25   |
| 3-16   | Bottom-hole temperatures during circulation and following shut-in for air circulation in the Baca well model. Flow rates of 270 scfm and 1090 scfm with soil conductivity values of 0.5 and 2.0 Btu/ft hr <sup>OF</sup> are shown . . . . .   | 27   |
| 3-17   | The wellbore geometry and undisturbed temperature gradient used in the Salton Sea well model calculations. . . . .  | 29   |
| 3-18   | Bottom-hole temperatures as a function of time during circulation and following shut-in at four flow rates for the Salton Sea well model . . . . .  | 30   |
| 3-19   | The downhole temperature profiles at times of 0, 2, 5, 10, 12, 16, and 24 hours following shut-in at four flow rates for the Salton Sea well model. . . . .   | 31   |
| 3-20   | The return temperatures at the surface in the annulus at four flow rates for the Salton Sea well model. . . . .   | 32   |

## LIST OF FIGURES

| Figure |   | Page |
|--------|---|------|
| 3-21   | Bottom-hole temperatures as a function of time during circulation and following shut-in at four flow rates for the Salton Sea well model using three casings in the wellbore. . . . .                                   | 34   |
| 3-22   | The downhole temperature profiles at times of 0, 2, 5, 10, 12, 16, and 24 hours following shut-in at four flow rates for the Salton Sea well model using three casings in the wellbore. . . . .                         | 35   |
| 3-23   | Bottom-hole temperatures as a function of time during circulation and following shut-in at four flow rates for the Salton Sea well model using a reduced tubing diameter in the wellbore. . . . .                       | 38   |
| 3-24   | The downhole temperature profiles at times of 0, 2, 5, 10, 12, 16, and 24 hours following shut-in at four flow rates for the Salton Sea well model using a reduced tubing diameter in the wellbore. . . . .             | 39   |
| 3-25   | Comparison of the radial temperature profiles for the standard wellbore and reduced tubing diameter case at flow rates of 100, 250, 500, and 1000 gpm. Temperatures are plotted at a depth of 1220 m (4000 ft). . . . . | 40   |
| 3-26   | The wellbore geometry and undisturbed temperature gradient used in the East Mesa well model calculations. . . . .   | 42   |
| 3-27   | Bottom-hole temperatures as a function of time during circulation and following shut-in at four flow rates for the East Mesa well model. . . . .  | 43   |
| 3-28   | The downhole temperature profiles at times of 0, 2, 5, 10, 12, 16, and 24 hours following shut-in at four flow rates for the East Mesa well model . . . .   | 44   |
| 3-29   | The wellbore geometry and undisturbed temperature gradient used in the Deep Salton Sea well model calculations . . . . .  | 47   |
| 3-30   | Bottom-hole temperatures as a function of time during circulation and following shut-in at four flow rates for the Deep Salton Sea well model. . . .  | 48   |
| 3-31   | The downhole temperature profiles at times of 0, 2, 5, 10, 12, 16, and 24 hours following shut-in at four flow rates for the Deep Salton Sea well model .   | 49   |

LIST OF TABLES

| Table |   | Page |
|-------|---|------|
| 3-1   | Baca Geothermal Area. Shut-in temperatures at the bottom of the hole for the standard wellbore case at circulation times of 1 and 20 days using water as the circulating fluid. . . . . | 6    |
| 3-2   | Comparison of midpoints of shut-in temperature curves for the Baca geothermal area for circulation times of 1 and 20 days . . . . .   | 18   |
| 3-3   | Baca Geothermal Area. Shut-in temperatures at the bottom of the hole for the standard wellbore case with mud as the circulating fluid. . . . .  | 21   |
| 3-4   | Salton Sea Geothermal Area. Shut-in temperatures at the bottom of the hole for three cases. . . . .   | 33   |
| 3-5   | Comparison of the midpoints of the shut-in temperature curves for the Salton Sea geothermal area well model for three cases . . . . .   | 36   |
| 3-6   | East Mesa Geothermal Area. Shut-in temperatures at the bottom of the hole . . . . .   | 41   |
| 3-7   | Salton Sea Geothermal Area Deep Well. Shut-in temperatures at the bottom of the hole . . . . .  | 46   |

## 1. INTRODUCTION

A large energy resource exists in the U.S. in the geothermal reservoirs which are primarily present in the western half of the country. However, developing these geothermal areas presents extreme problems for drilling and well logging operations due to the high temperatures reached down the hole. The maximum downhole temperature depends upon the specific geothermal area and the depth of the hole. For example, bottom-hole temperatures near 330°C are reached at a depth of 1800 m in the Baca KGRA (Known Geothermal Resource Area) while the same temperature occurs at 1400 m in the Salton Sea KGRA. Bentonite-based drilling muds form a high viscosity gel in the temperature range of 120 to 230°C, while downhole logging equipment has a typical maximum temperature limit near 175°C. Many geothermal well operations require some form of downhole cooling in order to be effective due to the lack of high temperature materials.

One method of wellbore cooling is circulating some fluid, such as water, mud or air, through the wellbore. Traeger, et al [1], performed a computer calculation for circulation in a hypothetical well in a magmahydrothermal region. They found that it was possible to cool the wellbore to below 200°C at a depth of 4.5 km, but the minimum attainable temperature increased as the well depth increased.

In this report the cooling effects due to fluid circulation in four well models are studied using the geothermal wellbore thermal simulator computer code GEOTEMP2 [3]. The well models used were slightly modified from those presented by Carson, Lin, and Livesay [2]. A brief description of the selected well models and of the computer code GEOTEMP2 is presented in Section 2. Section 3 contains the results of the computations on the four well models and on a parametric study of two of the well models. Finally, Section 4 summarizes the results of the computations and presents the conclusions obtained from this study.

## 2. WELL MODEL CALCULATIONS

Four well models have been chosen in this study to observe the effects of cooling by circulation upon the downhole wellbore temperatures. The descriptions of all but the deep Salton Sea well were obtained from the report on representative well models by Carson, Lin, and Livesay [2]. The four models are:

1. Baca model - This model was designed for the Baca KGRA located at the Baca Ranch, Valles Caldera in northern New Mexico. This well model provides an example of a moderately deep and hot geothermal reservoir.
2. Salton Sea model - This model was designed for the Salton Sea Geothermal Field located near the southeastern tip of the Salton Sea in southern California. An example of a shallow and hot reservoir is provided by this model.

3. East Mesa model - The East Mesa model was designed for the East Mesa KGRA which is located 30 miles east of El Centro, California, on the eastern edge of the Imperial Valley sedimentary basin. This model is an example of a deep and moderately hot reservoir.
4. Deep Salton Sea model - In this model a very deep and hot reservoir is simulated. The total hole depth is 5500 m (18,000 feet) with an estimated bottom hole temperature of 300°C (570°F).

For each of these well models a standard wellbore consisting of tubing to depth and four casing strings set to various depths with associated cemented and uncemented regions is described. The standard wellbore calculation simulates a one day circulation period using circulation rates of 100, 250, 500, 1000 gpm. For this standard case water was used as the circulating fluid. Following the one day circulation time at each water flow rate a shut-in (i.e. no flow) period of one day was implemented to observe the rate at which the wellbore warms. Computer calculations of the wellbore and soil temperatures for both circulation and shut-in periods were made at 1 hour intervals up to a time of 10 hours, then at times of 12, 16, 20, and 24 hours. Detailed descriptions of all the standard wellbores are presented in Section 3.

## 2.1 GEOTEMP2 COMPUTER CODE

The GEOTEMP2 computer code was used in this study to simulate fluid circulation in the well models. This code and the fluid flow and heat transfer equations and correlations employed have been treated in detail elsewhere [3,7,8]. The ability of this code to accurately predict temperatures down the wellbore has been evaluated previously [12]. Good agreement was found between the code predictions and field data. In this section only aspects of the code of special interest to this report will be discussed.

GEOTEMP2 employs a finite difference scheme to calculate heat transfer within and between the wellbore and the soil formation. A radial geometry is used by the code with the wellbore centerline as the origin of the coordinate system. Vertical grid size is constant and was set at 61 m (200 ft) for these calculations. The size of the grids in the radial direction is not constant but exponentially increases away from the wellbore centerline. Ten grids are used in the radial direction with the tenth grid set at a distance of 15 m (50 ft) from the centerline. This last grid defines the boundary conditions for the temperature and is set at the undisturbed temperature gradient of the specific geothermal area. The first three radial grids define the wellbore. The first grid contains the tubing, the second grid consists of the annulus, and the third grid contains the region consisting of all the casing, cemented intervals, and, finally, the beginning of the soil formation.

As with any computer code, certain assumptions and limitations are inherent in the implementation of the code. Some of the assumptions and limitations of GEOTEMP2 are:

- 1) Forced and natural convection of the fluid is only treated within the tubing and the annulus; only heat conduction is treated in the grids located in the soil formation.
- 2) Only radial heat conduction is treated in the tubing and the annulus; vertical heat conduction is assumed negligible compared to convection because of the larger grid size in the vertical direction compared to the radial direction.
- 3) All casings are assumed to extend to the surface from the setting depth.
- 4) The cemented interval outside of a casing is not required to extend to the surface. Fluid is contained in the annuli between the casings where the casings are not cemented. This fluid was chosen to be the same as the circulating fluid for all the calculations except for the gas circulation case in the Baca well model. For this case, water was placed in the uncemented casing annuli.

5) Radiative heat transfer in the wellbore and soil is assumed to be negligible.

6) Initial conditions: Fluid temperatures in the tubing and annulus are initially set at the geothermal gradient temperature values.

For turbulent flow in a pipe, the rate of heat transfer between a flowing fluid and a solid is given by the general expression [11]:

$$Nu = C Re^m r^n , \quad (2-1)$$

where C is a shape factor which depends on the geometry of the system, and m and n are constants, dependent on the system geometry, which typically lie in the range:  $0.5 < m < 0.8$  and  $0.3 < n < 0.4$  [11].

Nu is the Nusselt number given by

$$Nu = \frac{hd}{k} , \quad (2-2)$$

where h is the convection or heat transfer coefficient, d is the pipe diameter, and k is the thermal conductivity of the fluid. The Nusselt number is a measure of the rate of heat flow at a fluid/solid interface. The Reynolds number, Re, is given by

$$Re = \frac{\rho vd}{\mu} , \quad (2-3)$$

where  $\rho$  is the fluid density,  $\mu$  is the fluid viscosity, and v is the flow velocity. Finally, the Prandtl number, Pr, which is the ratio of the velocity to the temperature diffusion is given by

$$Pr = \frac{\mu C_p}{k} , \quad (2-4)$$

where  $C_p$  is the specific heat capacity. The heat transfer coefficient, h, is thus a complicated function of the fluid properties and flow geometry. This point must be kept in mind when reviewing the results of the calculations presented in this report.

### 3. WELL MODEL RESULTS

In this section the results of the calculations performed on the four well models are presented. Results are first discussed for the standard wellbore case which, for the Baca well model, also includes the effect of different soil thermal conductivities. Next, results are presented on any parametric study performed on the particular well model.

#### 3.1 BACA WELL MODEL

The standard wellbore description and geothermal profile for the Baca well model is illustrated in Figure 3-1. Total well depth was 1830 m (6000 ft). A 20-inch casing reached a depth of 61 m (200 ft) and was cemented to the surface. A 13-3/8-inch casing extended to 457 m (1500 ft) and was also cemented to the surface. A third casing of 9-5/8 inches reached a depth of 914 m (3000 ft) and was cemented from the bottom of the casing up to a depth of 762 m (2500 ft). Finally, the fourth 7-inch casing extended to the bottom of the hole at 1830 m (6000 ft). 5.5-inch tubing was used in this simulation.

The undisturbed geothermal profile consisted of two linear temperature components [10]. The first linear profile extends from the surface (set nominally at 21°C (70°F) to a depth of 975 m (3200 ft) where the temperature was fixed at 260°C (500°F). The second temperature profile begins at this depth and extends to the bottom of the hole where the temperature was set at 327°C (620°F).

##### 3.1.1 STANDARD WELLBORE CALCULATIONS AND RESULTS

For the Baca KGRA three soil conductivities were used to observe the effect of different soil conductivity values on the rate of heat transfer and hence on the wellbore temperature profile. The soil conductivity,  $k$ , is a function of the rock type, rock porosity and water saturation, and temperature. A suitable range for basalt is 0.4 to 1.5 Btu/ft hr °F (1.5 to  $6.0 \times 10^{-3}$  cal/cm s C) [9]. Calculations were done at three values of  $k$ : 0.5, 1.0, and 2.0 Btu/ft hr °F. Figure 3-2 shows the results of the computer calculations for the four flow rates and three soil conductivities. In this figure the temperatures plotted were those which were calculated for a point inside the tubing at the bottom of the hole. The temperature cooling due to circulation and the temperature warming following shut-in are illustrated.

The shut-in temperature profiles are shown in Figures 3-3, 3-4, and 3-5 for  $k=0.5$ , 1.0, and 2.0 Btu/ft hr °F, respectively. The shut-in temperatures at the bottom of the hole and inside the tubing are tabulated in Table 3-1.

# WELLBORE GEOMETRY AND GEOTHERMAL GRADIENT FOR THE BACA KGRA

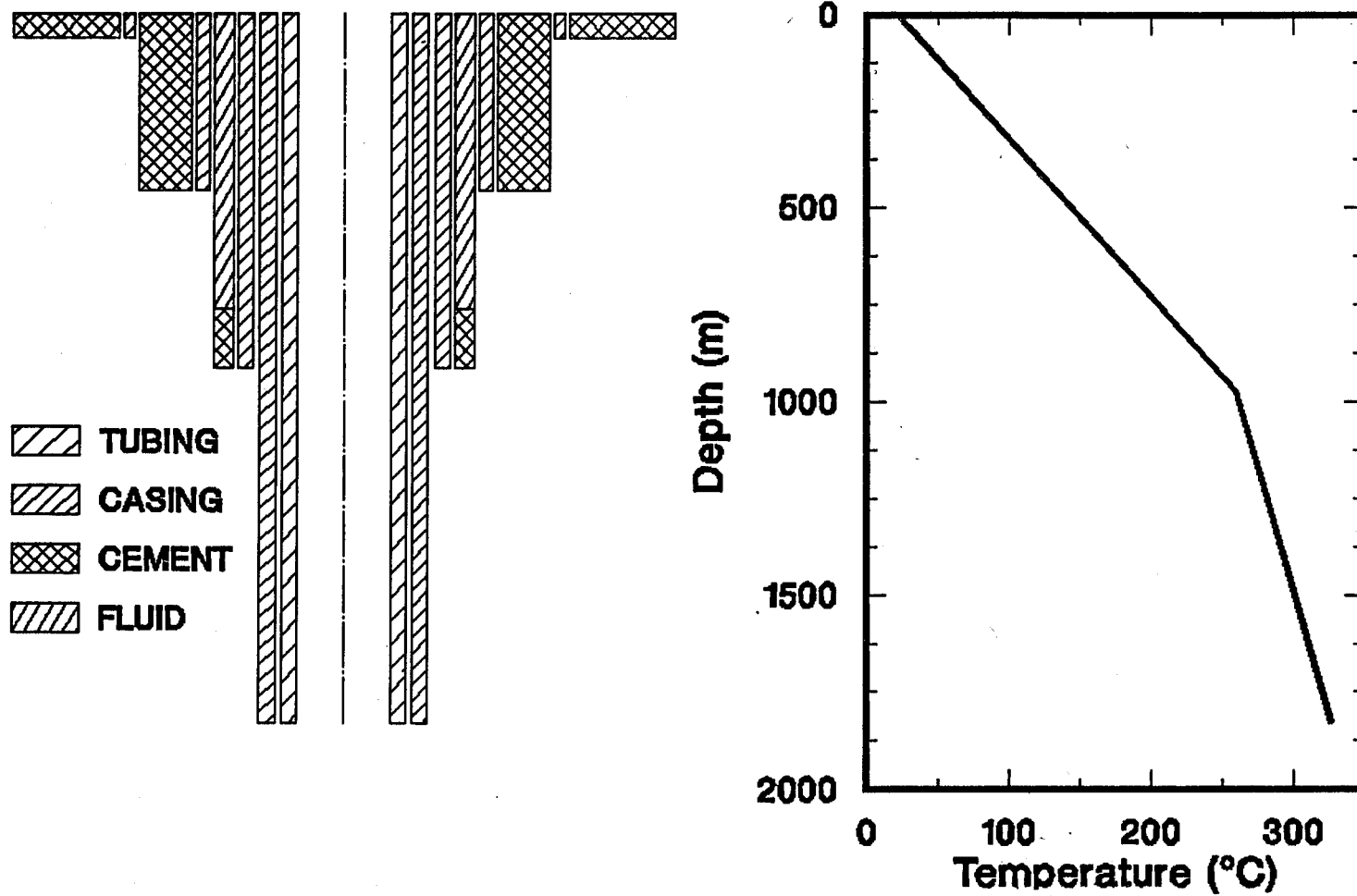


Figure 3-1. The wellbore geometry and undisturbed temperature gradient used in the Baca well model calculations.

7  
Temperature (°C)

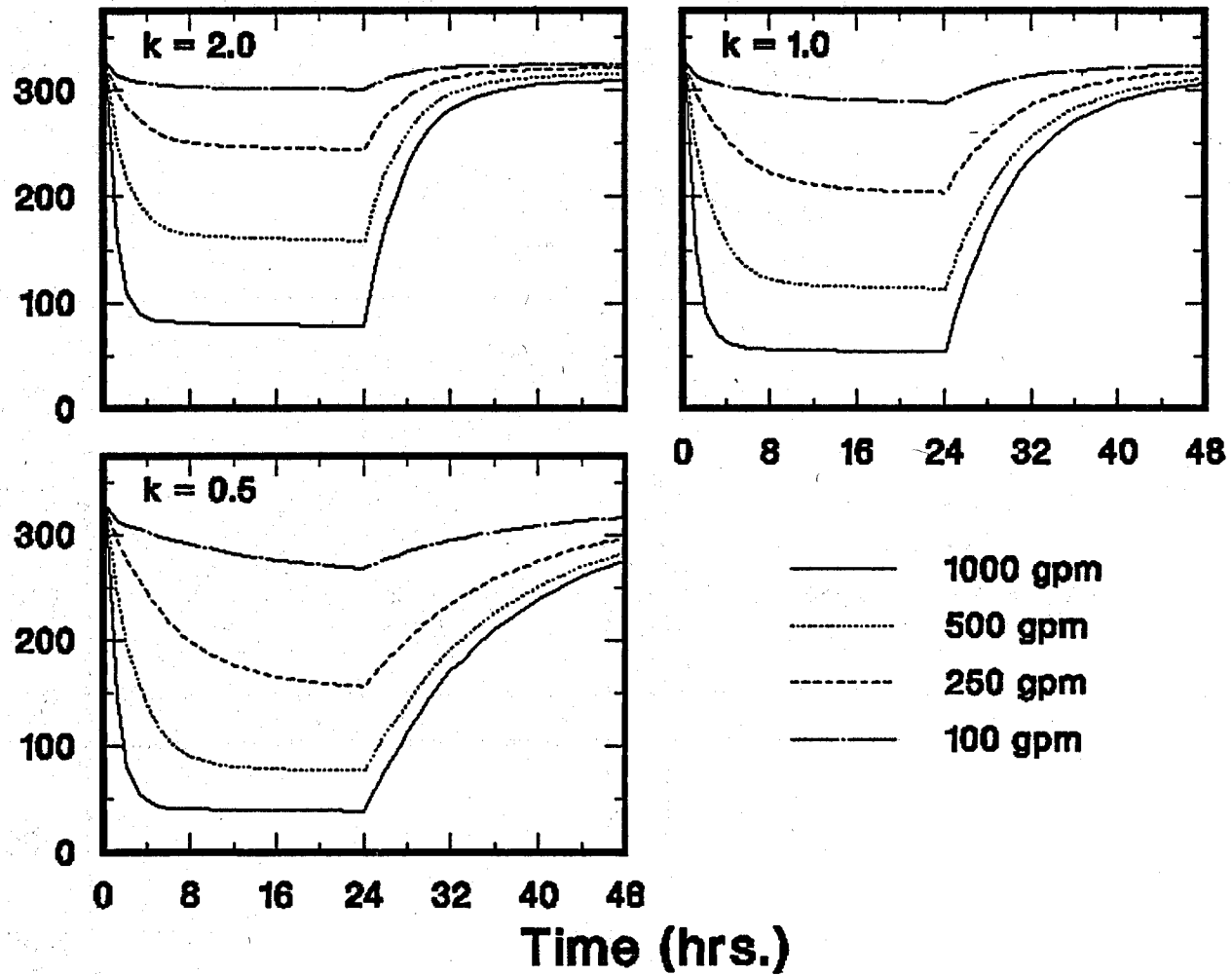


Figure 3-2. Bottom-hole temperatures as a function of time during circulation and following shut-in at four flow rates and three soil conductivities for the Baca well model.  $k$  is the soil thermal conducting units of Btu/ft hr °F.

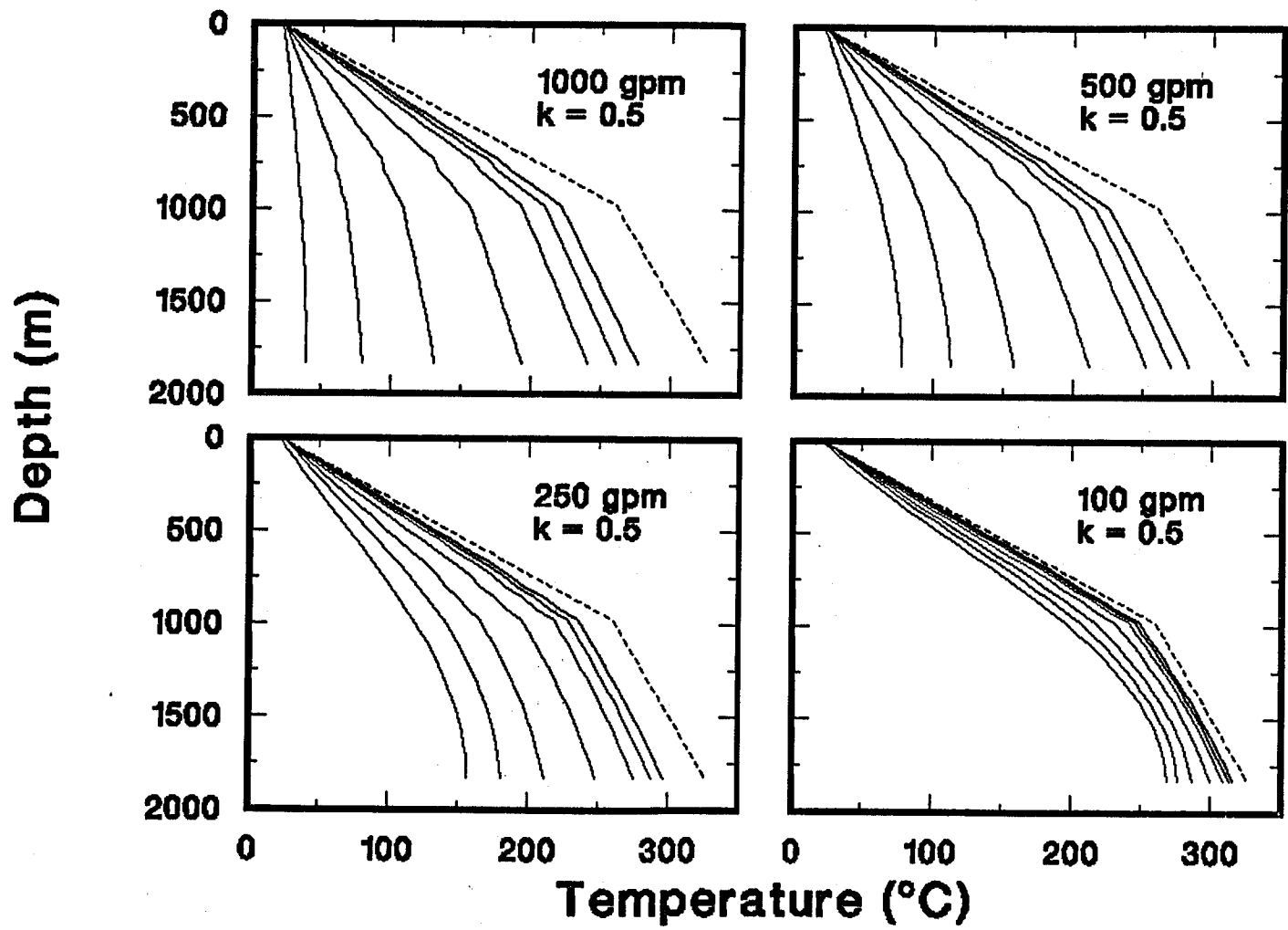


Figure 3-3. The downhole temperature profiles inside the tubing at times of 0, 2, 5, 10, 12, 16, and 24 hours following shut-in at four flow rates and a soilthermal conductivity of 0.5 Btu/ft hr<sup>o</sup>F for the Baca well model. The dashed line is the undisturbed temperature gradient.

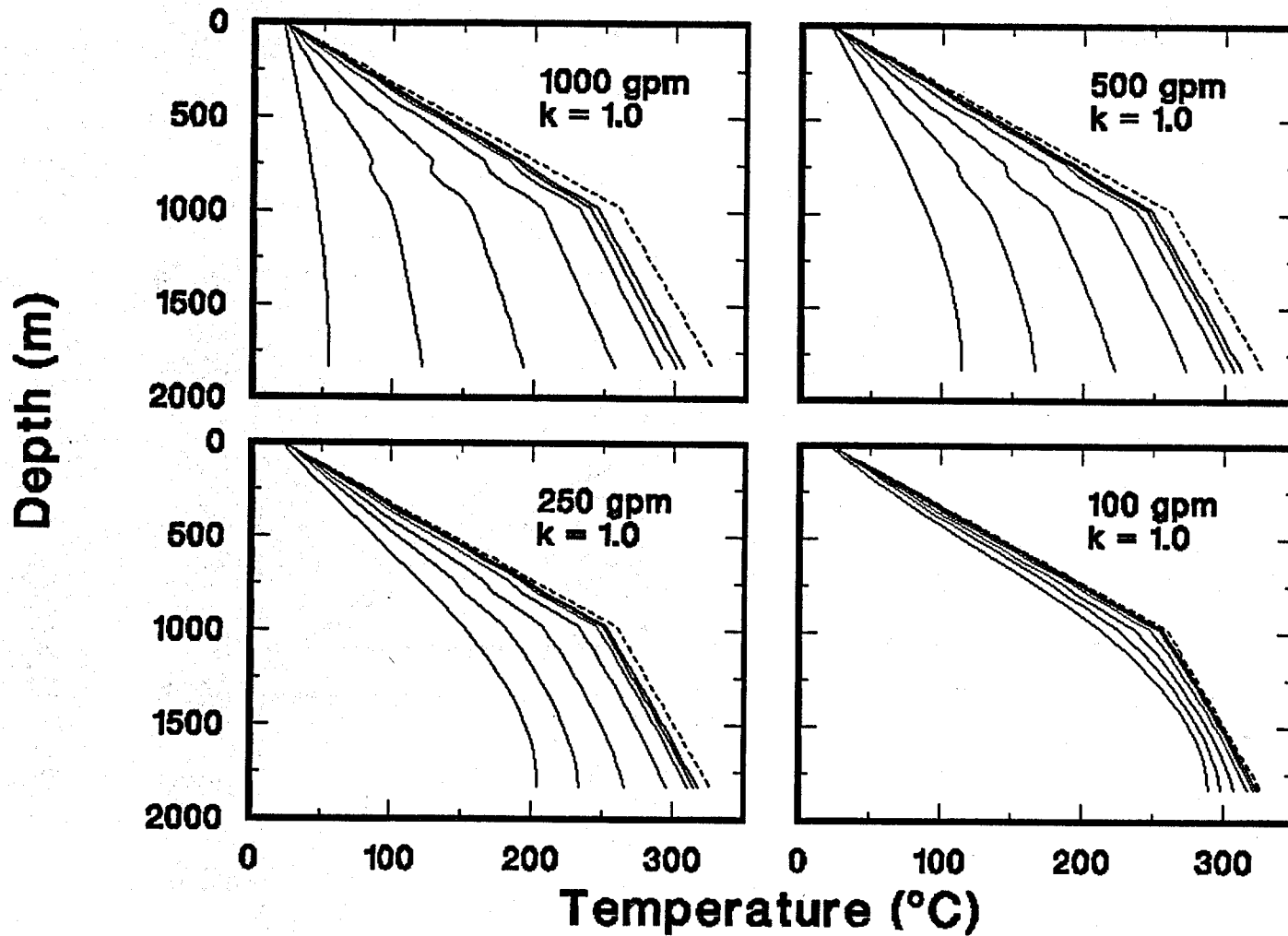


Figure 3-4. The downhole temperature profiles inside the tubing at times of 0, 2, 5, 10, 12, 16, and 24 hours following shut-in at four flow rates and a soil thermal conductivity of 1.0 Btu/ft hr  $^{\circ}\text{F}$  for the Baca well model. The dashed line is the undisturbed temperature gradient.

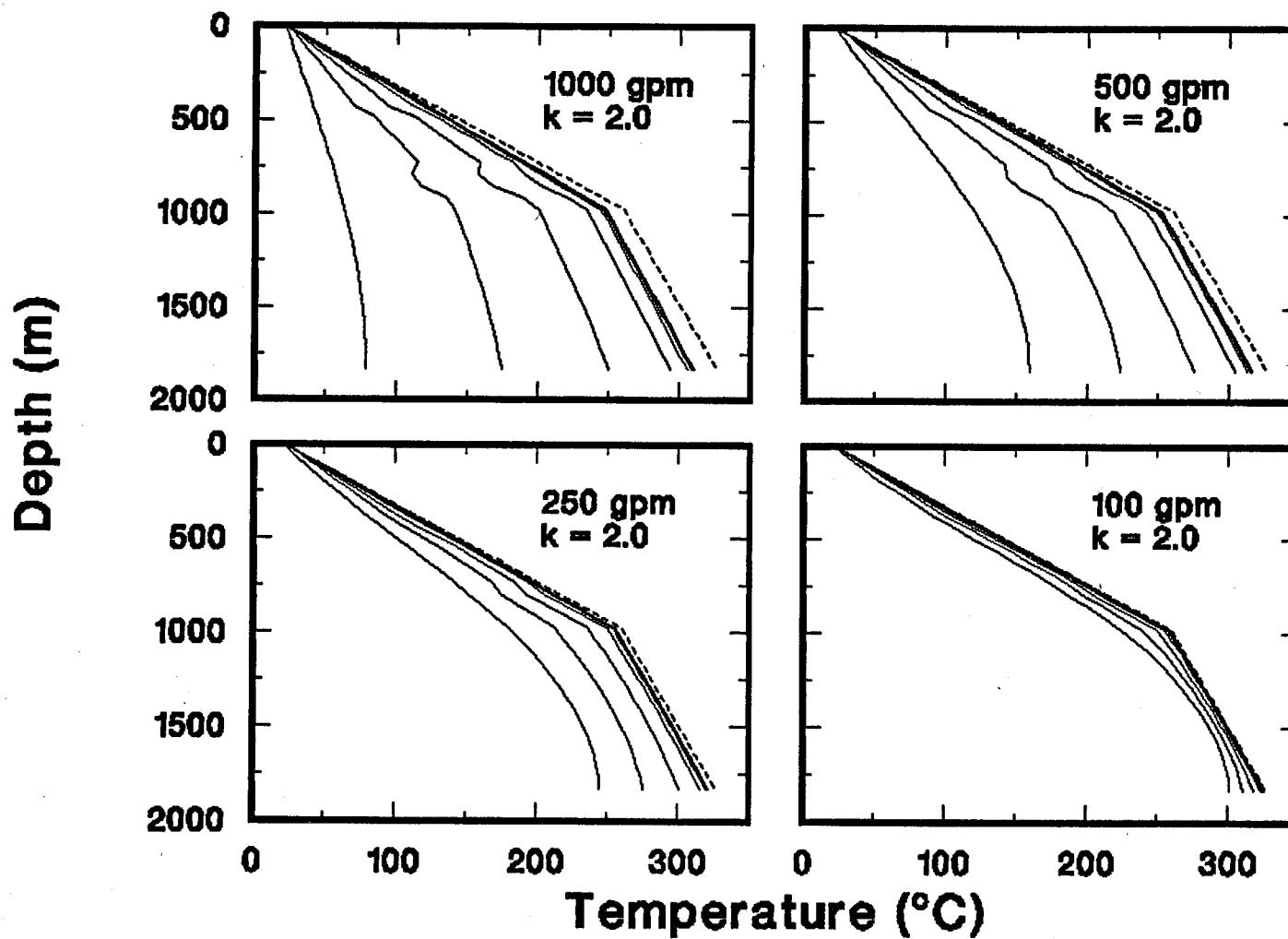


Figure 3-5. The downhole temperature profiles inside the tubing at times of 0, 2, 5, 10, 12, 16, and 24 hours following shut-in at four flow rates and a soil thermal conductivity of 2.0 Btu/ft hr  $^{\circ}\text{F}$  for the Baca well model. The dashed line is the undisturbed temperature gradient.

Table 3-1. Baca Geothermal Area. Shut-in temperatures at the bottom of the hole for the standard wellbore case at circulation times of 1 and 20 days using water as the circulating fluid. The soil thermal conductivity,  $k$ , is in units of Btu/ft hr °F.

| Flow Rate<br>(gpm) | Circ.<br>Time | $k$ | Shut-in Temperatures, °C, at |     |     |     |     |     |           |
|--------------------|---------------|-----|------------------------------|-----|-----|-----|-----|-----|-----------|
|                    |               |     | 0                            | 1   | 2   | 5   | 10  | 16  | 24 (hrs.) |
| 1000               | 1 day         | 2.0 | 78                           | 131 | 174 | 251 | 293 | 306 | 310       |
|                    |               | 1.0 | 54                           | 89  | 121 | 192 | 257 | 290 | 307       |
|                    |               | 0.5 | 39                           | 59  | 79  | 131 | 193 | 240 | 276       |
| 500                | 1 day         | 2.0 | 159                          | 194 | 223 | 275 | 304 | 313 | 316       |
|                    |               | 1.0 | 113                          | 141 | 166 | 222 | 272 | 298 | 311       |
|                    |               | 0.5 | 77                           | 94  | 112 | 157 | 211 | 269 | 283       |
| 250                | 1 day         | 2.0 | 244                          | 262 | 276 | 301 | 316 | 320 | 321       |
|                    |               | 1.0 | 204                          | 220 | 234 | 266 | 295 | 311 | 318       |
|                    |               | 0.5 | 157                          | 169 | 181 | 211 | 248 | 288 | 297       |
| 100                | 1 day         | 2.0 | 301                          | 306 | 311 | 318 | 323 | 324 | 325       |
|                    |               | 1.0 | 289                          | 293 | 298 | 308 | 317 | 321 | 324       |
|                    |               | 0.5 | 269                          | 273 | 277 | 287 | 299 | 313 | 316       |
| 1000               | 20 days       | 2.0 | 66                           | 106 | 139 | 198 | 233 | 245 | 251       |
|                    |               | 0.5 | 37                           | 53  | 70  | 112 | 163 | 202 | 232       |
| 250                | 20 days       | 2.0 | 226                          | 241 | 254 | 277 | 291 | 296 | 298       |
|                    |               | 0.5 | 139                          | 149 | 160 | 188 | 221 | 257 | 266       |

In Figure 3-2 it is evident that the cooling effect increases as the flow rate increases and as the soil conductivity decreases. The shapes of both the cooling and warming curves change as  $k$  decreases tending to become much more gradual in their approach to an asymptotic limit. The figures all show that the 100 gpm flow rate is ineffective in cooling the wellbore at all soil conductivities. The 250 gpm flow rate cools the bottom-hole below 200°C only for  $k=0.5$  Btu/ft hr °F, while the 500 and 1000 gpm flow rates are effective in cooling the wellbore to a reasonably low value at all soil conductivities.

For  $k=0.5$  Btu/ft hr °F shown in Figure 3-3, all of the flow rates except for 100 gpm have bottom-hole temperatures slightly above or below 200°C up to 5 hours after shut-in. The bottom-hole temperatures for both the 1000 gpm and 500 gpm flow rates remain below about 200°C after 10 hours. Only the 1000 gpm flow rate produces a bottom-hole temperature less than 260°C (500°F) after 20 hours of shut-in.

The downhole temperature profiles for  $k=1.0$  Btu/ft hr °F are shown in Figure 3-4. The bottom-hole temperatures for 250, 500, and 1000 gpm are all less than or equal to about 230°C (446°F) after 2 hours. At 5 hours the bottom-hole temperature for the 1000 gpm flow rate is still below 200°C

while the 500 gpm flow rate shows a temperature somewhat above 200°C having a value of 222°C (432°F). After 10 hours of shut-in, all the flow rates have bottom-hole temperatures above 250°C (482°F) and only the temperatures for the 1000 gpm and 500 gpm flow rates are near 260°C (500°F).

In Figure 3-5, which shows the temperature profiles down the hole after shut-in for  $k=2.0$  Btu/ft hr °F, only a flow rate of 1000 gpm cools the well below 200°C after 2 hours. At 5 hours after shut-in, the bottom-hole temperature approaches 260°C (500°F). For the 500 gpm flow rate, the temperature is just below 200°C after 1 hour and warms to 275°C (527°F) after 5 hours of shut-in.

The results shown here demonstrate that the most effective cooling is obtained for high flow rates and low soil thermal conductivity. The soil thermal conductivity was considered to be a constant in this analysis. In reality  $k$  depends on the rock type, temperature, rock permeability and porosity and the thermal conductivity of the saturating fluid. In general, the thermal conductivity of rocks would be expected to decrease with increased temperatures [13]. It should be noted that only heat conduction was treated in the soil formation. The presence of convective transport processes will alter the temperature distributions.

The water return temperature at the surface through the annulus is presented in Figure 3-6. The temperature of the fluid at the surface in the annulus is a function of the flow velocity, the heat transfer rate, and the temperature difference between the fluid in the annulus and the fluid in tubing and the temperature of the surrounding soil. For  $k=2.0$  Btu/ft hr °F and flow rates of 250 and 500 gpm, the same steady-state temperature is reached while a lower temperature, almost as low as for the 1000 gpm flow rate, is reached for a flow rate of 100 gpm. It does appear that as  $k$  decreases, the curves begin to approach an expected pattern, i.e. a pattern where lower steady-state temperatures are achieved at higher flow rates. This is probably due to the fact that the lower soil thermal conductivity allows less heat to be transferred from the soil to the fluid. Hence, the fluid temperature at higher flow rates would be reduced. Note that the curves for the 100-gpm flow do not change significantly as  $k$  is changed. This implies that the amount of heat absorbed at this flow rate has reached a steady-state value.

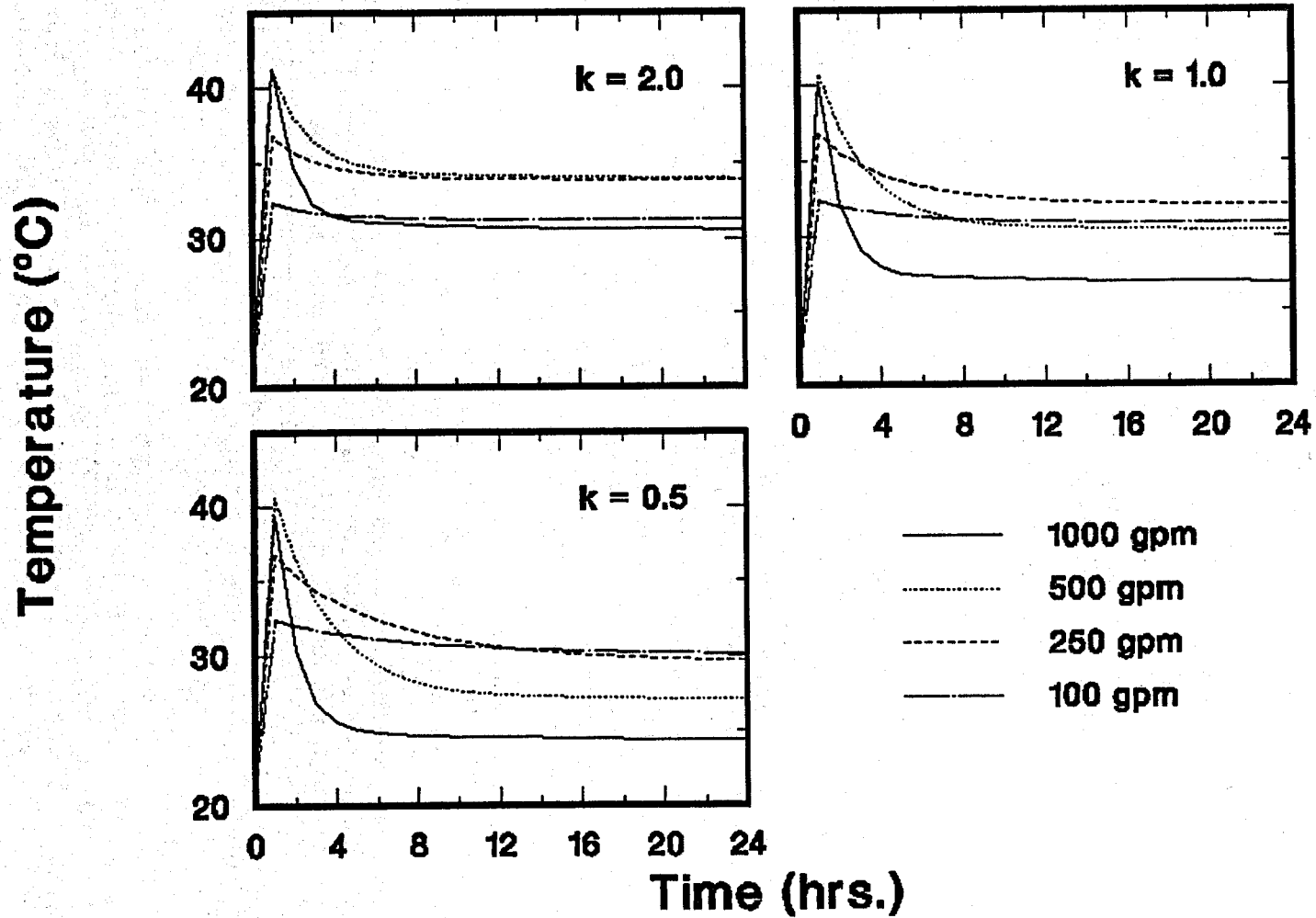


Figure 3-6. The return temperatures at the surface in the annulus at four flow rates and three soil thermal conductivities for the Baca well model.

### 3.1.2 PARAMETRIC STUDY OF THE BACA WELL MODEL

In the standard wellbore calculations, the soil thermal conductivity was varied to observe its effect upon the computed downhole temperatures. In this section the results of the variation of the water circulation time and circulating fluid are discussed. A circulation time of 20 days, rather than one day as in the preceding section, was used with flow rates of 250 and 1000 gpm. Two changes were made in the circulating fluid. First, a mud with a viscosity of 15 cp (water has a viscosity of 1 cp) but with the same density as water was used in calculations at the same flow rates and soil conductivities as the previously described calculations with water. Second, air was used as the circulating fluid with mass flow rates comparable to water flow rates of 250 and 1000 gpm.

#### 20 DAY CIRCULATION TIME

The temperatures at bottom hole after shut-in are compared for water circulation times of 1 and 20 days at flow rates of 250 and 1000 gpm and soil conductivities of 0.5 and 2.0 Btu/ft hr °F in Figure 3-7. The corresponding downhole temperatures after shut-in for  $k=0.5$  and  $k=2.0$  Btu/ft hr °F are illustrated in Figures 3-8 and 3-9, respectively. As expected, cooler temperatures are observed for the longer circulation time. Table 3-1 summarizes the temperatures at selected times following shut-in. Note that the minimum temperature after circulation is surprisingly similar for both the 1 and 20 day circulation times. After 1 day of circulation, the final temperatures for a flow rate of 1000 gpm are 78 and 39°C at  $k=2.0$  and  $k=0.5$  Btu/ft hr °F, respectively, compared to values of 66 and 37°C for the 20-day circulation time. Somewhat greater differences are observed for the lower flow rate of 250 gpm. Here, final temperatures are 244 and 157°C at  $k=2.0$  and  $k=0.5$  Btu/ft hr °F, respectively, at 1000 gpm versus 226 and 139°C at 250 gpm.

The primary effect of longer circulation time is the delay experienced in warming the wellbore. In Figure 3-7 and from Table 3-1, the temperatures after 24 hours of shut-in are noticeably cooler for the 20-day circulation time. At a flow rate of 1000 gpm the temperature difference is near 40°C while at 250 gpm the difference is 20 to 30°C. Table 3-2 shows how the curve shape has changed with circulation time by tabulating the midpoints of the shut-in temperature curves (i.e. the temperatures and times corresponding to:  $(T(24 \text{ hrs}) + T(0 \text{ hrs}))/2$ ; this temperature corresponds to the mean temperature of the fluid during the 24-hour shut-in period). Note that the curve midpoints for the 20-day circulation time occur at lower temperatures but at about the same times as in the 1-day circulation case.

For  $k=0.5$  Btu/ft hr °F and a 1000-gpm flow rate, the bottom-hole temperature is 202°C (396°F) at 16 hours after shut-in for the 20-day circulation time and is only 232°C (450°F) after 24 hours. For the flow rate of 250 gpm, temperatures are significantly warmer with temperatures less than 200°C (392°F) at 5 hours following shut-in and less than 260°C (500°F) at 20 hours.

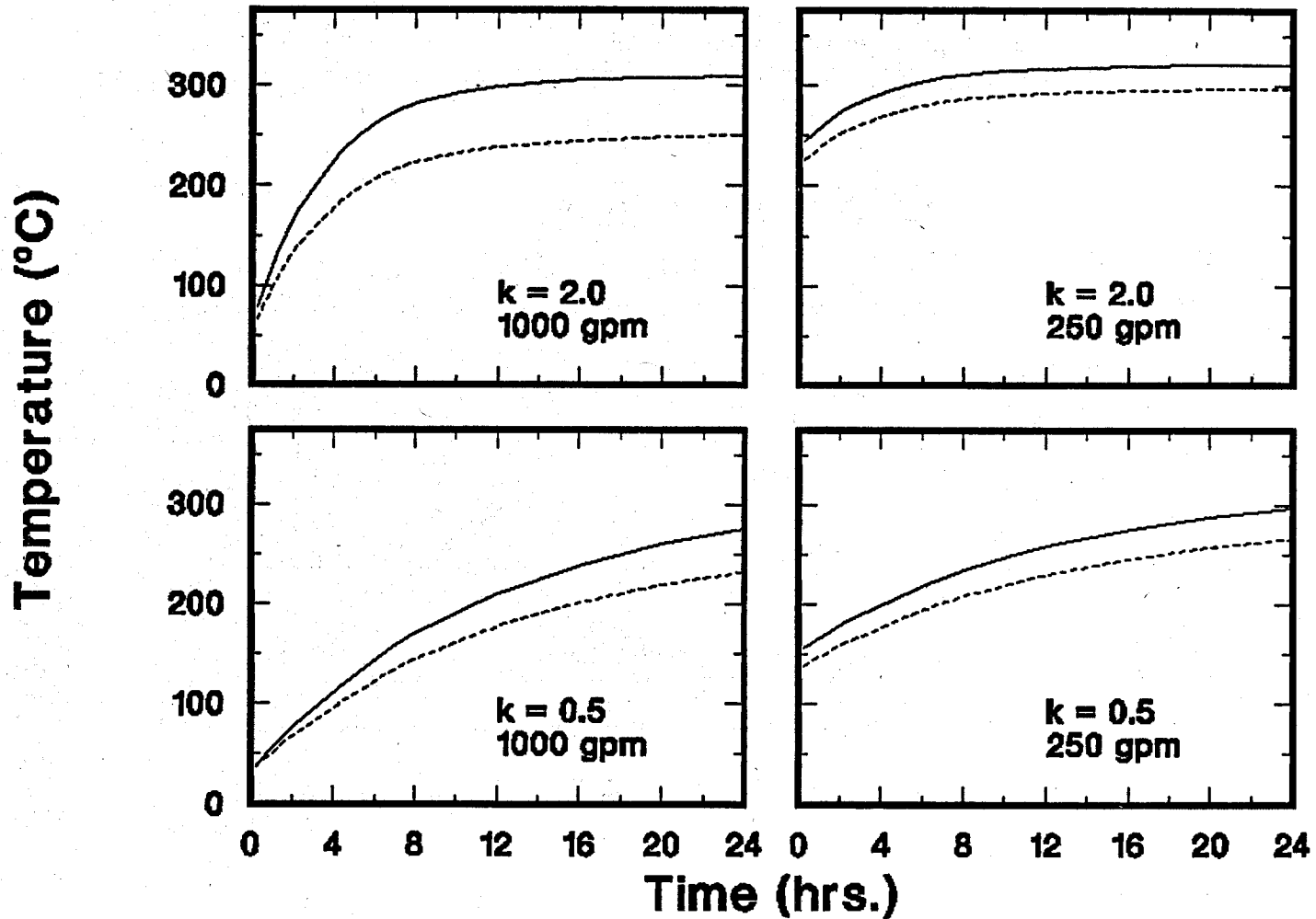


Figure 3-7. Comparison of the bottom-hole temperatures following shut-in for circulation times of 1 and 20 days at flow rates of 250 and 1000 gpm and soil thermal conductivities of 0.5 and 2.0 Btu/ft hr °F. The dashed lines are the temperatures for the 20-day circulation time.

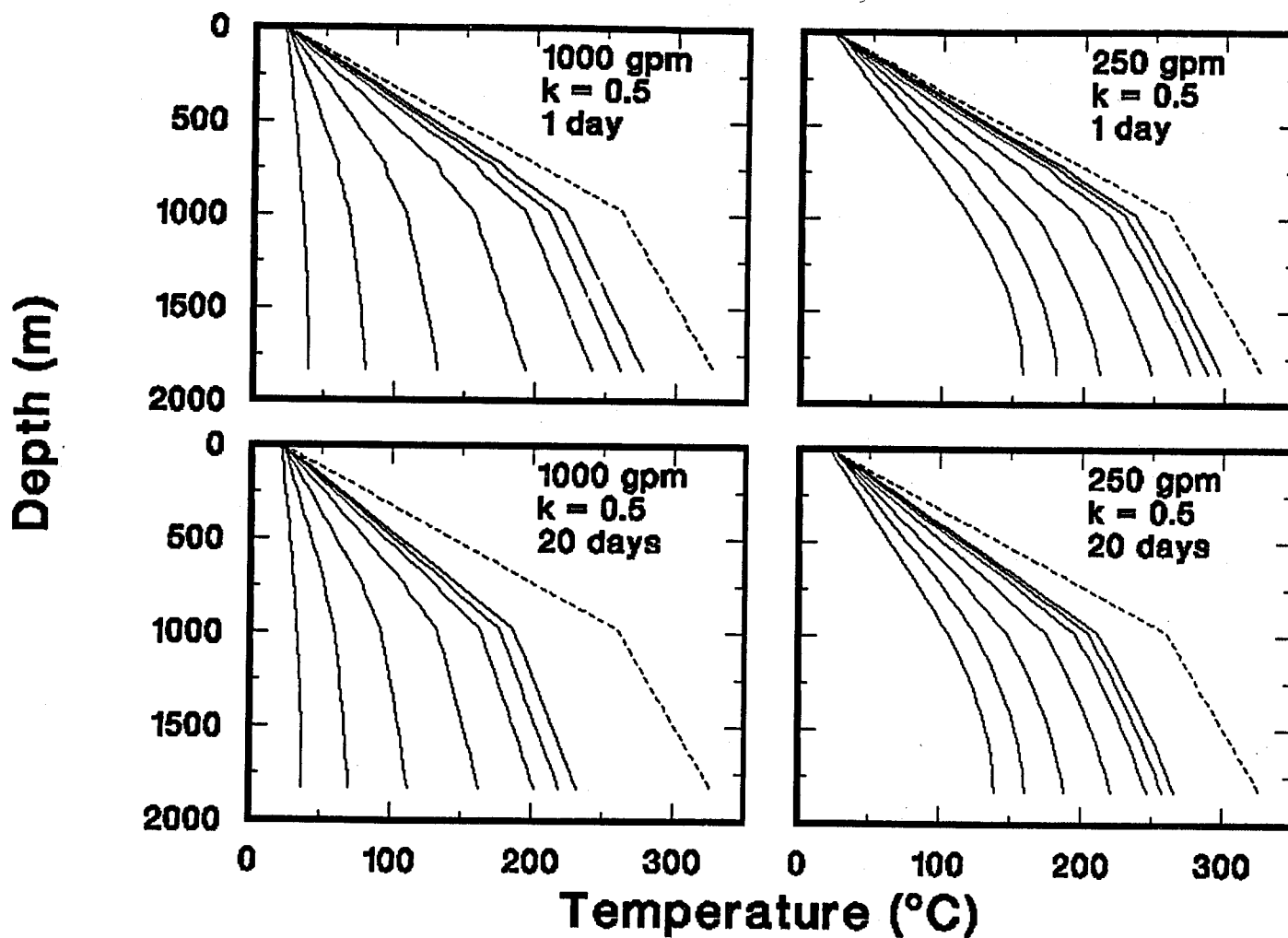


Figure 3-8. Comparison of the downhole temperatures inside the tubing at times of 0, 2, 5, 10, 12, 16, and 24 hours following shut-in at circulation times of 1 and 20 days for flow rates of 250 and 1000 gpm and a soil thermal conductivity of 0.5 Btu/ft hr<sup>o</sup>F for the Baca well model. The dashed line is the undisturbed temperature gradient.

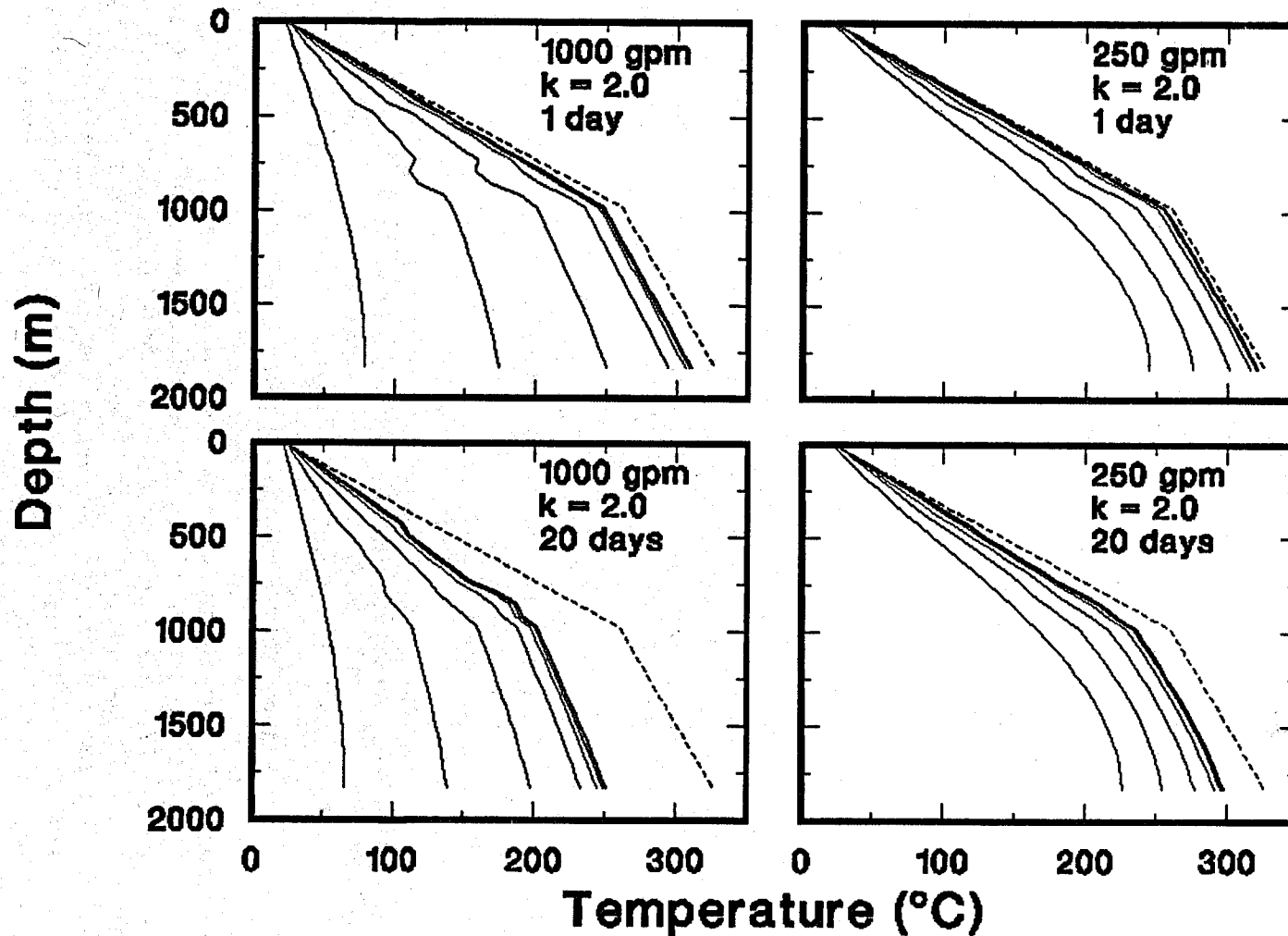


Figure 3-9. Comparison of the downhole temperatures inside the tubing at times of 0, 2, 5, 10, 12, 16, and 24 hours following shut-in at circulation times of 1 and 20 days for flow rates of 250 and 1000 gpm and a soil thermal conductivity of 2.0 Btu/ft hr °F for the Baca well model. The dashed line is the undisturbed temperature gradient.

Table 3-2. Comparison of midpoints of shut-in temperature curves for the Baca geothermal area for circulation times of 1 and 20 days. The soil conductivity, k, is in units of Btu/ft hr °F.

| Flow Rate (gpm) | Circ. Time | k   | Mid-point temp. (°C) | Approx. time (hrs.) |
|-----------------|------------|-----|----------------------|---------------------|
| 1000            | 1 day      | 2.0 | 194                  | 3                   |
|                 | 20 days    |     | 159                  | 3                   |
|                 | 1 day      | 0.5 | 158                  | 7                   |
|                 | 20 days    |     | 135                  | 7                   |
| 250             | 1 day      | 2.0 | 283                  | 2                   |
|                 | 20 days    |     | 262                  | 3                   |
|                 | 1 day      | 0.5 | 227                  | 8                   |
|                 | 20 days    |     | 203                  | 8                   |

For a soil conductivity of 2.0 Btu/ft hr °F and a 1000-gpm flow rate, the temperature is slightly less than 200°C (392°F) after 5 hours of shut-in. At 10 hours, the temperature is 233°C (451°F) compared to 293°C (559°F) for a 1-day circulation time. The differences between 1 and 20-day circulation times is only on the order of 20°C for the 250-gpm flow rate.

Radial temperature profiles are shown at selected depths for 1 and 20 days of circulation at flow rates of 250 and 1000 gpm for  $k = 0.5$  Btu/ft hr °F in Figure 3-10 and for  $k = 2.0$  Btu/ft hr °F in Figure 3-11. As expected, cooler soil temperatures are obtained at a greater distance from the wellbore for the 20-day circulation time. At a distance of only 3 m, the soil temperature is at about the undisturbed value even for the 20-day calculations. Reducing the soil thermal conductivity, as can be observed by comparing Figures 3-10 and 3-11, reduces the penetration distance of the cooling effect due to the circulating fluid.

#### MUD AS THE CIRCULATING FLUID

The circulation and shut-in temperatures calculated for the Baca Well Model using a mud with a viscosity of 15 cp and the same density as water are plotted in Figure 3-12. The corresponding downhole temperature profiles for  $k=1.0$  Btu/ft hr °F are presented in Figure 3-13. Comparing these plots with Figures 3-2 and 3-4 for the corresponding water circulation case, it is quite obvious that the larger mud viscosity has a pronounced effect upon the downhole temperatures. Table 3-3 lists the bottom-hole temperatures after shut-in for mud circulation.

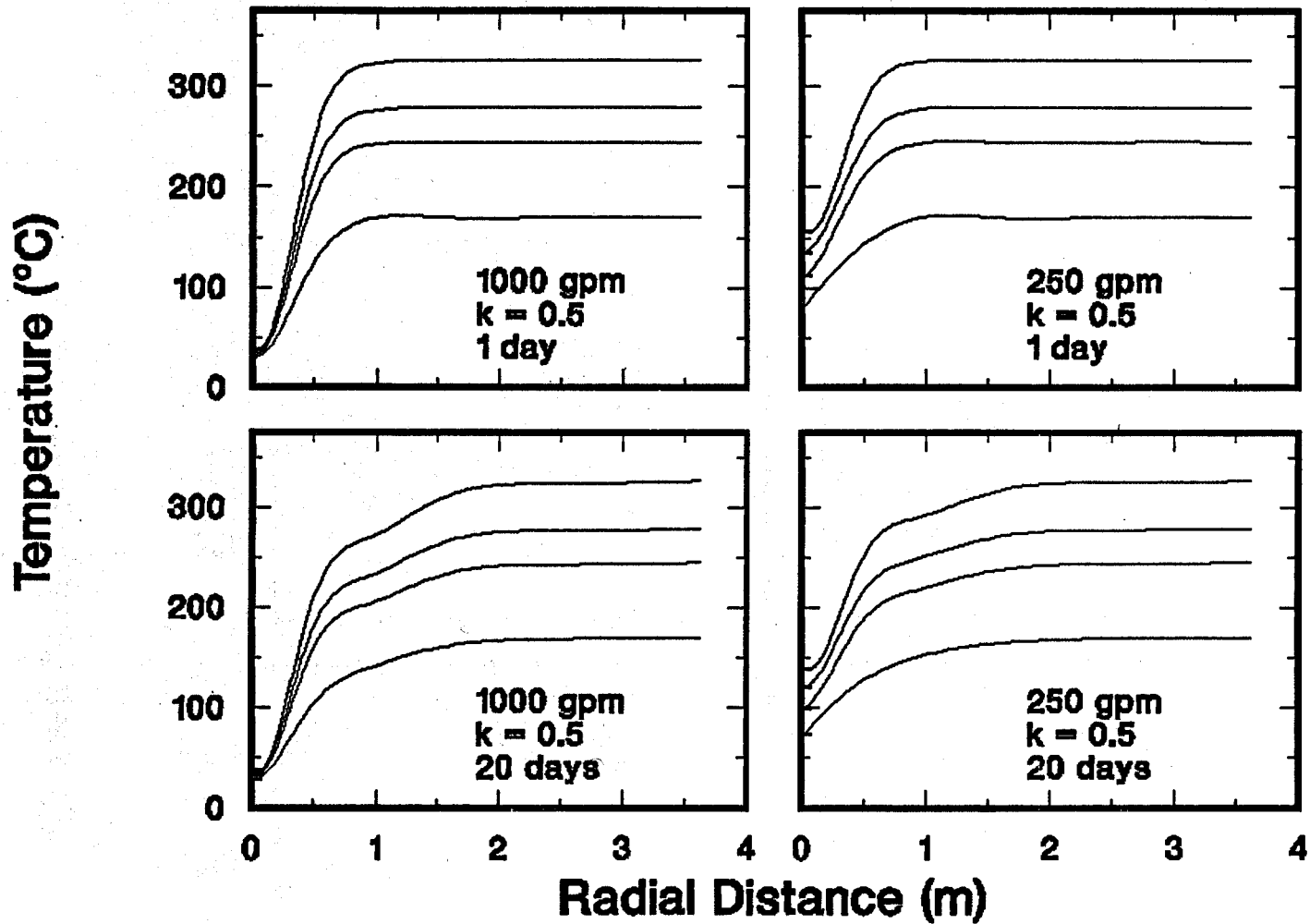


Figure 3-10. Comparison of the radial temperature profiles for circulation times of 1 and 20 days at flow rates of 250 and 1000 gpm and a soil thermal conductivity of 0.5 Btu/ft hr °F. Temperatures are plotted at depths of 610 m (2000 ft), 914 m (3000 ft), 1220 m (4000 ft), and 1830 m (6000 ft).

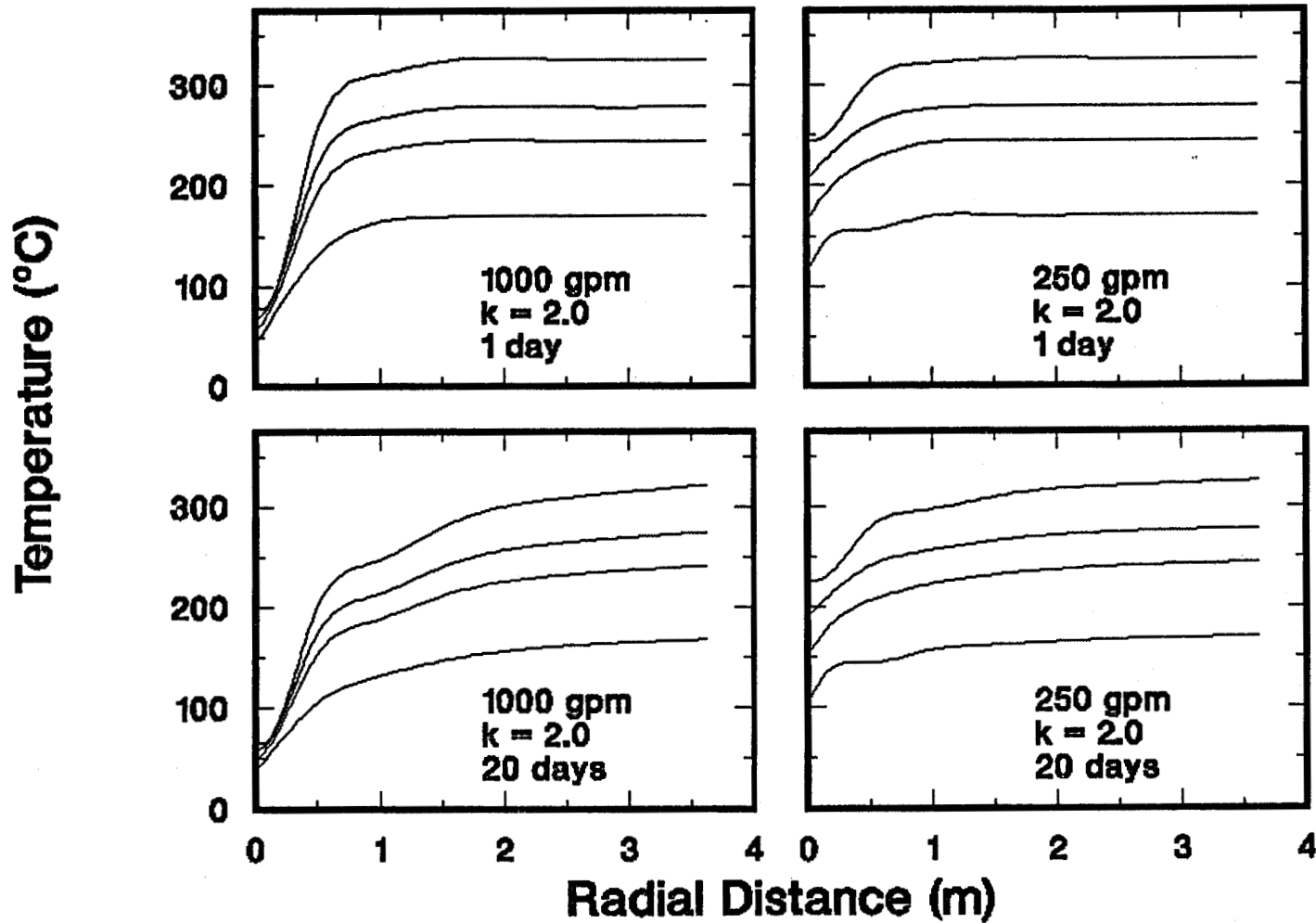


Figure 3-11. Comparison of the radial temperature profiles for circulation times of 1 and 20 days at flow rates of 250 and 1000 gpm and a soil thermal conductivity of 2.0 Btu/ft hr °F. Temperatures are plotted at depths of 610 m (2000 ft), 914 m (3000 ft), 1220 m (4000 ft), and 1830 m (6000 ft).

Table 3-3. Baca Geothermal Area. Shut-in temperatures at the bottom of the hole for the standard wellbore case with mud as the circulating fluid.

| Flow Rate<br>(gpm) | k   | Shut-in Temperatures, °C, at |     |     |     |     |     |           |
|--------------------|-----|------------------------------|-----|-----|-----|-----|-----|-----------|
|                    |     | 0                            | 1   | 2   | 5   | 10  | 16  | 24 (hrs.) |
| 1000               | 2.0 | 54                           | 101 | 146 | 229 | 283 | 302 | 309       |
|                    | 1.0 | 41                           | 70  | 102 | 175 | 244 | 283 | 303       |
|                    | 0.5 | 32                           | 49  | 68  | 120 | 183 | 232 | 271       |
| 500                | 2.0 | 98                           | 137 | 175 | 245 | 290 | 306 | 312       |
|                    | 1.0 | 69                           | 96  | 124 | 190 | 253 | 287 | 306       |
|                    | 0.5 | 48                           | 64  | 83  | 132 | 191 | 237 | 274       |
| 250                | 2.0 | 163                          | 192 | 218 | 268 | 300 | 312 | 316       |
|                    | 1.0 | 119                          | 142 | 164 | 217 | 267 | 295 | 310       |
|                    | 0.5 | 82                           | 97  | 113 | 156 | 208 | 249 | 281       |
| 100                | 2.0 | 244                          | 258 | 271 | 296 | 313 | 319 | 322       |
|                    | 1.0 | 206                          | 219 | 232 | 263 | 292 | 308 | 317       |
|                    | 0.5 | 159                          | 169 | 181 | 210 | 246 | 273 | 296       |

The mud tends to be cooler than the water under similar conditions. The reason for this is apparent by inspecting Eqn. 2-1, which relates the Nusselt number to the Reynolds and Prandtl numbers for turbulent flow. The heat transfer coefficient (which is contained within the dimensionless Nusselt number) depends on the fluid viscosity in a complicated manner. Careful analysis of this expression shows that as the viscosity increases the heat transfer rate decreases. Hence, the high viscosity mud is less effective at removing heat from the soil than water and as a result has a lower temperature than water. This conclusion can be demonstrated by looking at the radial temperature profiles for mud and water at the four flow rates as shown in Figure 3-14. Water is shown to produce lower temperatures in the formation especially at the lower flow rates. This effect does not extend a significant distance away from the wellbore.

The observed temperature differences between the mud and water circulation cases are most pronounced at the lower flow rates of 100 and 250 gpm. The downhole temperatures at the 100-gpm rate for mud, shown in Figure 3-13, are less than 300°C (572°F) up to 10 hours after shut-in, whereas the temperatures remain below 300°C only up to 2 hours for water circulation.

The return temperatures at the surface for mud circulation are plotted in Figure 3-15. Note that the temperatures follow the expected trend; higher flow rates produce lower surface temperatures. This is in sharp contrast to the confusing situation observed for water circulation in Figure 3-6.

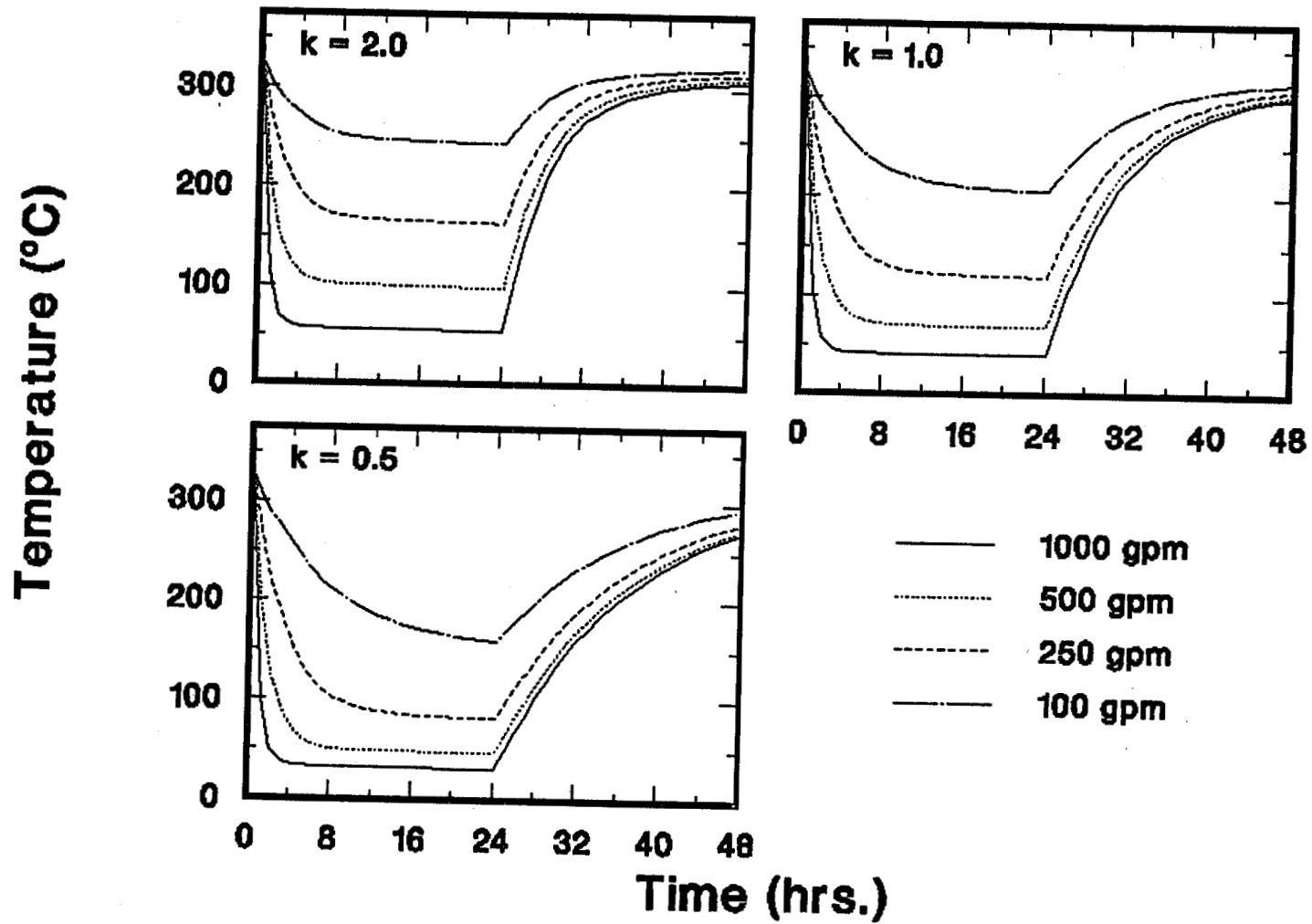


Figure 3-12. Bottom-hole temperatures as a function of time during circulation and following shut-in at four flow rates and three soil conductivities for the Baca well model using mud as the circulating fluid.

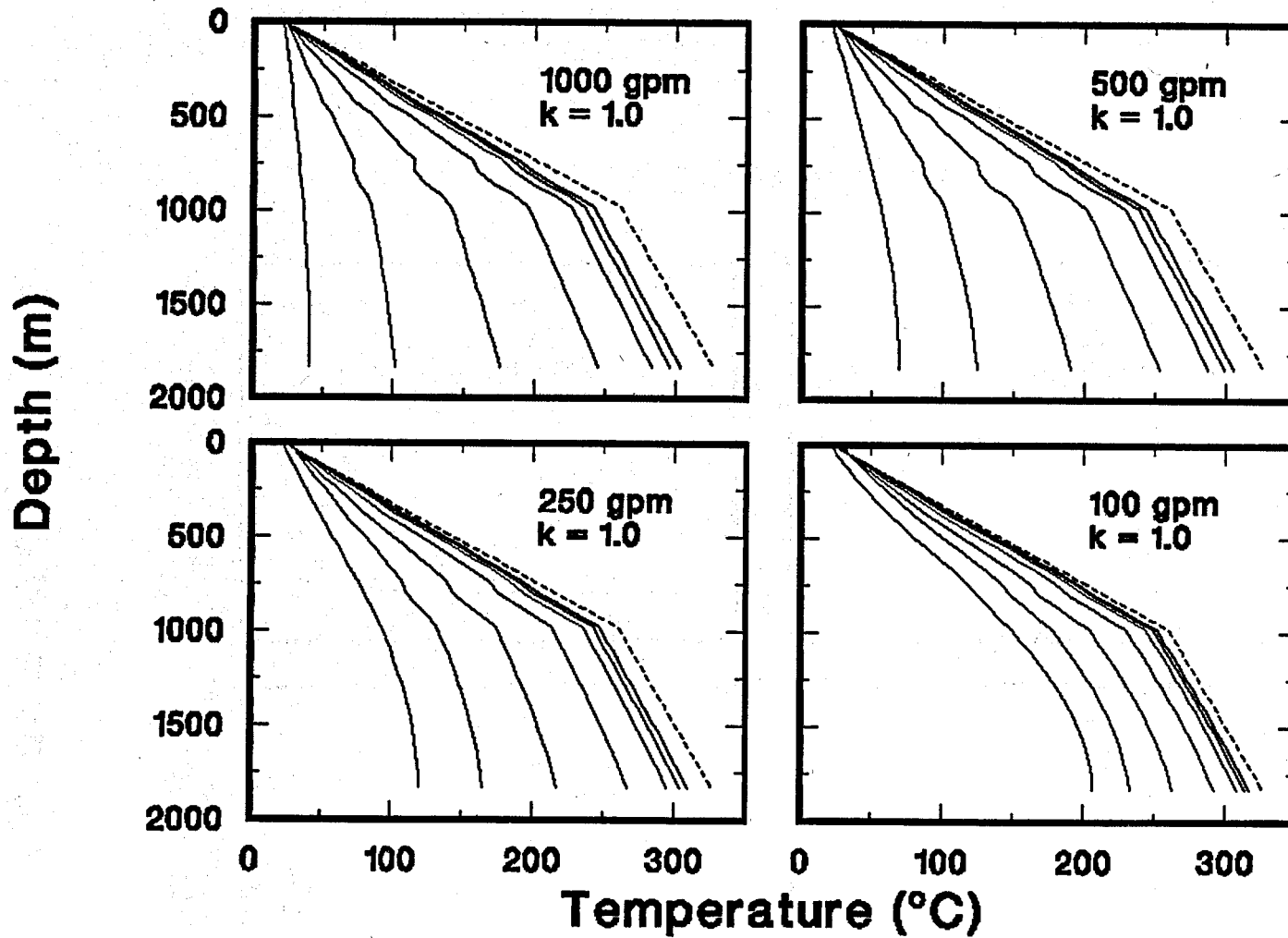


Figure 3-13. The downhole temperature profiles inside the tubing at times of 0, 2, 5, 10, 12, 16, and 24 hours following shut-in at four flow rates and a soil thermal conductivity of 1.0 Btu/ft hr °F for the Baca well model using mud as the circulating fluid. The dashed line is the undisturbed temperature gradient.

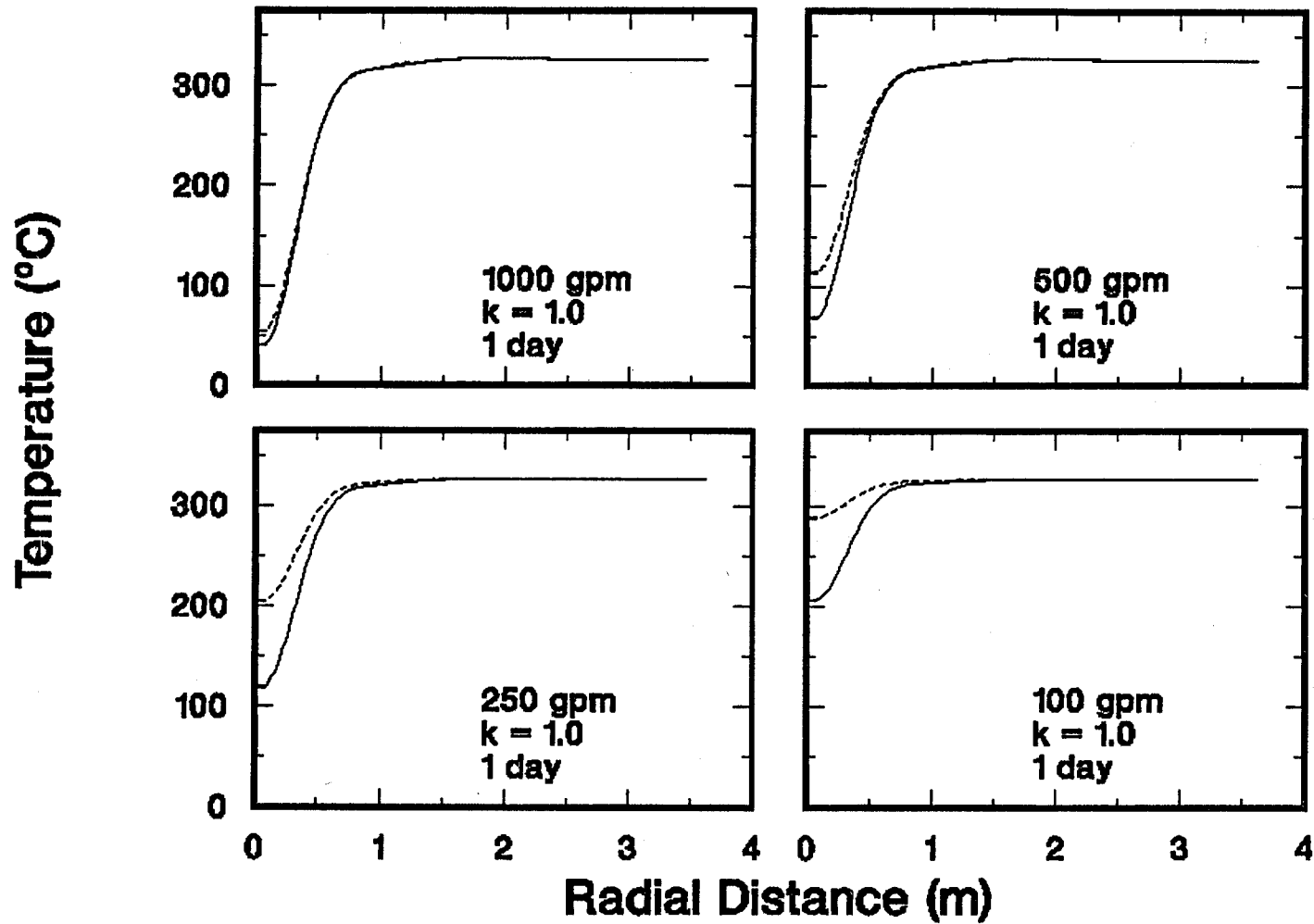


Figure 3-14. Comparison of the radial temperature profiles for circulation with water (solid line) or mud (dashed line). The bottom-hole temperatures are plotted. The soil thermal conductivity is 1.0 Btu/ft hr °F.

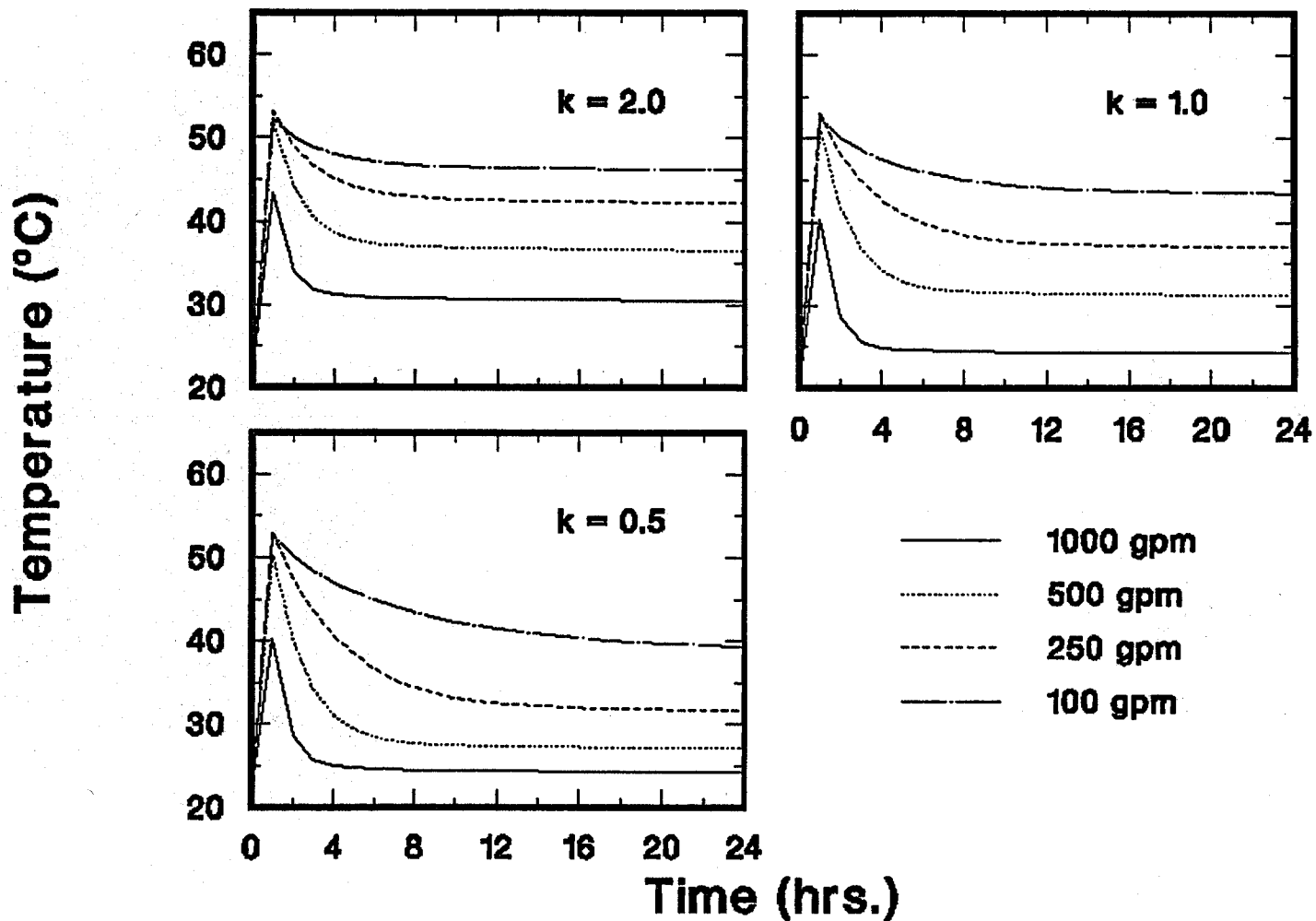


Figure 3-15. The return temperatures at the surface in the annulus at four flow rates and three soil thermal conductivities for the Baca well model using mud as the circulating fluid.

## AIR AS THE CIRCULATING FLUID

Air was tested as a cooling agent by simulating circulation in the wellbore. Figure 3-16 summarizes the results of the computer calculations using air at flow rates of 1090 scfm and 270 scfm which correspond to the mass flow rates of water at 1000 gpm and 250 gpm, respectively. The standpipe pressure was set to 1500 psi in order to obtain the desired mass flow rates. Figure 3-16 clearly shows that air is a very ineffective fluid for wellbore cooling. The bottom-hole temperatures are significantly higher, greater than 320°C (608°F), than for the corresponding water case which had temperatures less than 100°C for the 1000-gpm flow rate and less than 250°C for the 250-gpm flow rate at shut-in. A lower soil thermal conductivity also has little effect on the downhole temperatures.

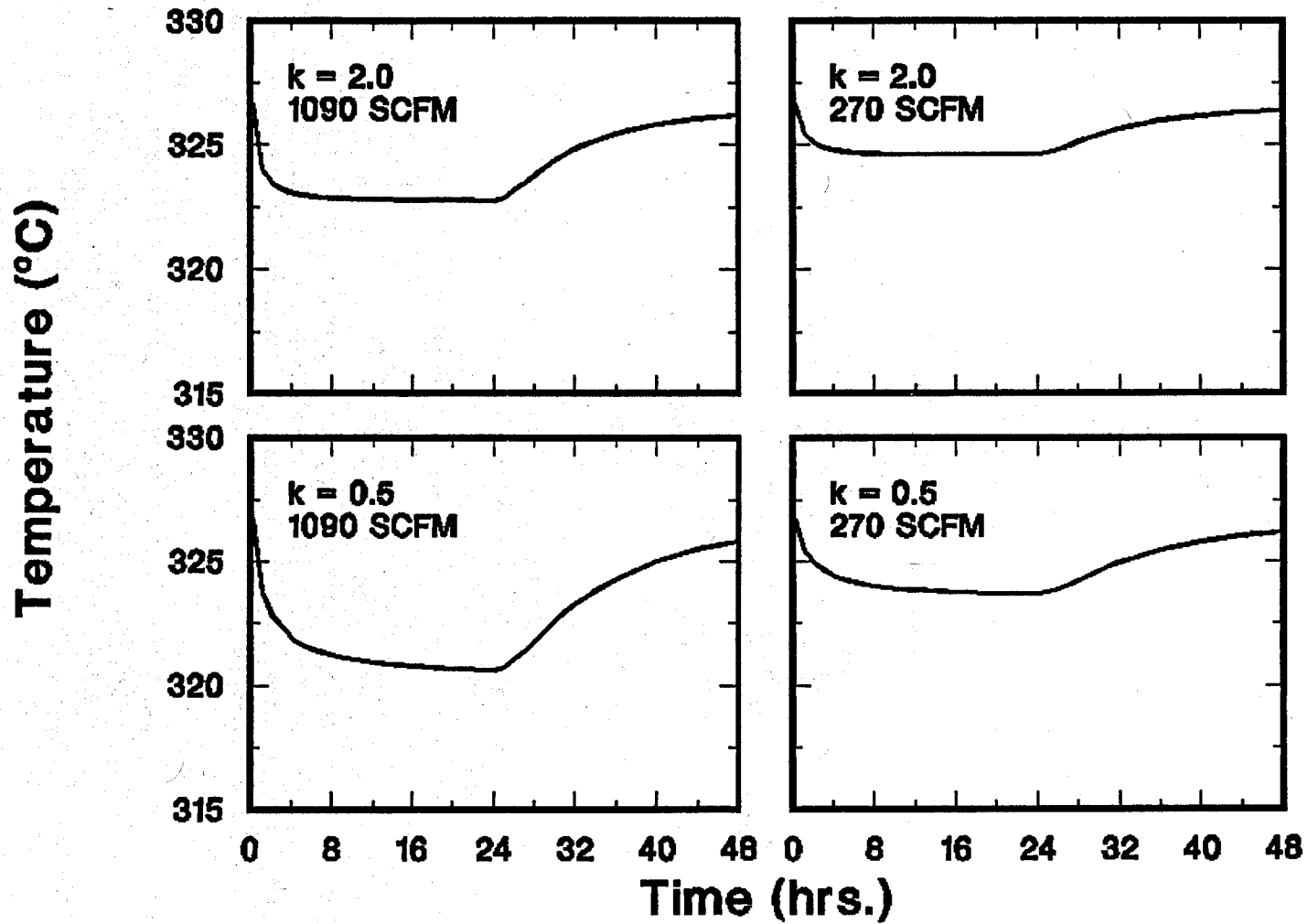


Figure 3-16. Bottom-hole temperatures during circulation and following shut-in for air circulation in the Baca well model. Flow rates of 270 scfm and 1090 scfm with soil conductivity values of 0.5 and 2.0 Btu/ft hr °F are shown.

### 3.2 SALTON SEA WELL MODEL

The standard wellbore description and geothermal profile for the Salton Sea well model is illustrated in Figure 3-17. Total well depth was 1370 m (4500 ft). A 20-inch casing reached a depth of 183 m (600 ft) and was cemented to the surface. A 13-3/8-inch casing extended to 396 m (1300 ft) and was also cemented to the surface. A third casing of 9-5/8 inches reached a depth of 914 m (3000 ft) and was cemented from the bottom of the casing up to a depth of 335 m (1100 ft). Finally, the fourth 7-inch casing extended to the bottom of the hole at 1370 m (4500 ft). 5.5-inch tubing was used in this simulation.

The undisturbed geothermal profile consisted of two linear temperature components [4]. The first linear profile extends from the surface (set nominally at 21°C (70°F) to a depth of 747 m (2450 ft) where the temperature was fixed at 288°C (550°F). The second temperature profile begins at this depth and extends to the bottom of the hole where the temperature was set at 332°C (630°F).

#### 3.2.1 STANDARD WELLBORE CALCULATIONS AND RESULTS

The soil thermal conductivity at the Salton Sea KGRA is near 1.2 Btu/ft hr °F [4], therefore, only a value of  $k=1.0$  Btu/ft hr °F has been used in the calculations. The temperatures during water circulation and following shut-in are shown in Figure 3-18 for the four flow rates of 100, 250, 500, 1000 gpm. The shut-in temperature profiles are given in Figure 3-19. These figures show that, as in the case for the Baca well model, the cooling effect of the circulating fluid increases as the flow rate is increased. The 100-gpm flow rate seems particularly ineffective in providing any cooling compared to all the higher flow rates.

Table 3-4 lists the bottom-hole temperatures at various times after shut-in. The flow rate of 250 gpm cools the fluid inside the tubing to 178°C (352°F) after 1 day of circulation, however, the water quickly warms to greater than 260°C (500°F) 5 hours after shut-in. For both the flow rates of 500 and 1000 gpm, the fluid temperatures remain below 250°C (482°F) at 5 hours after shut-in. At 10 hours following shut-in, the fluid temperatures are still below 290°C (554°F). The shut-in temperatures observed here are similar to those obtained for the Baca well model for  $k=1.0$  Btu/ft hr °F except that the minimum temperature achieved at the bottom of the hole is less than for the corresponding Baca case and the temperatures tend to rise more rapidly. Both of these results can be attributed to the shallower well depth used for the Salton Sea model compared to the Baca well model.

The water return temperature in the annulus at the surface is presented in Figure 3-20. These temperatures show behavior similar to that found for the Baca well model in Figure 3-6. Both the 100-gpm and 250-gpm flow rates reach the same steady-state temperature at the surface. The lowest return temperature of near 27°C (80°F) is observed for the 1000-gpm flow rate.

## WELLBORE GEOMETRY AND GEOTHERMAL GRADIENT FOR THE SALTON SEA KGRA

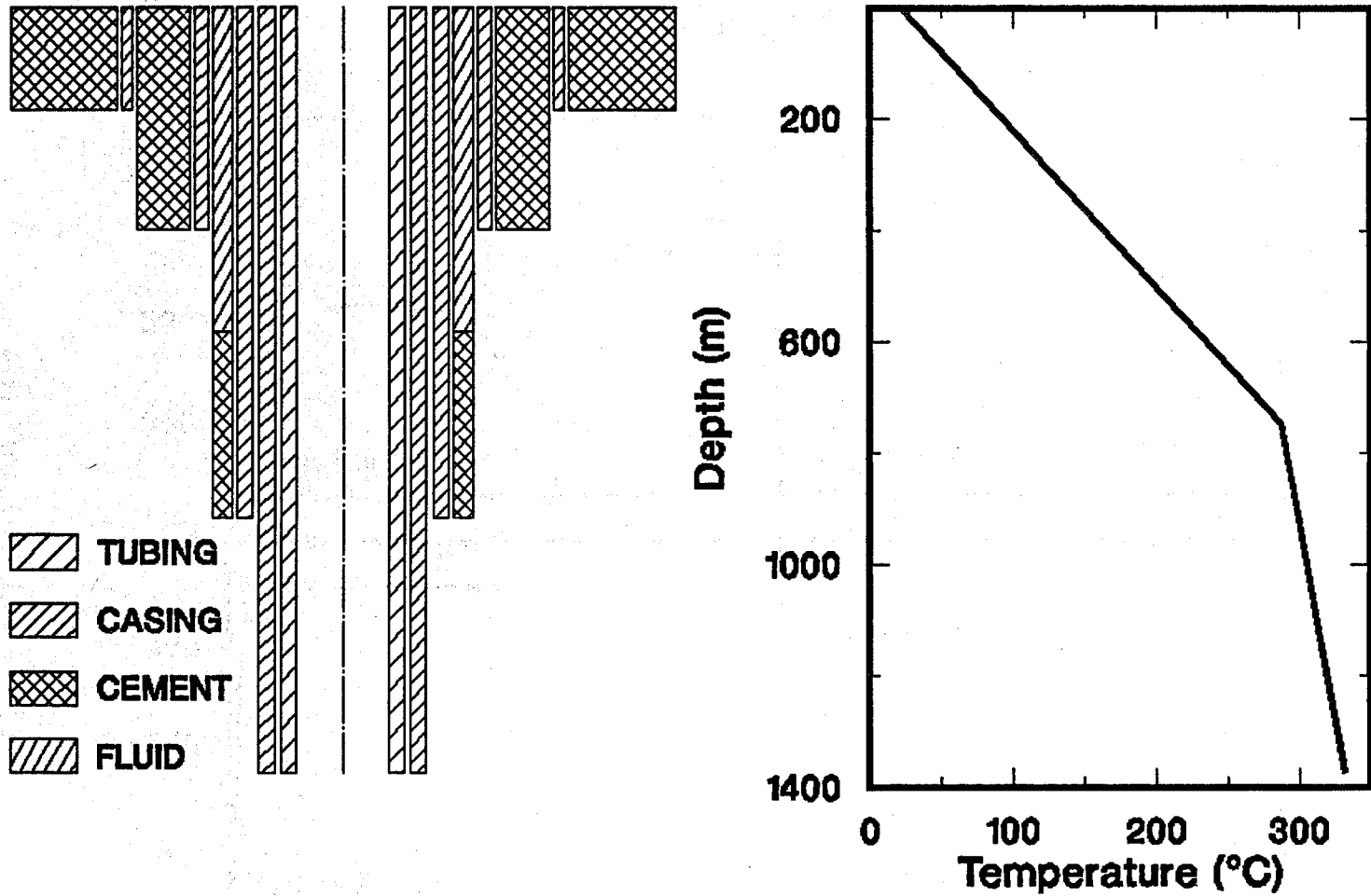


Figure 3-17. The wellbore geometry and undisturbed temperature gradient used in the Salton Sea well model calculations.

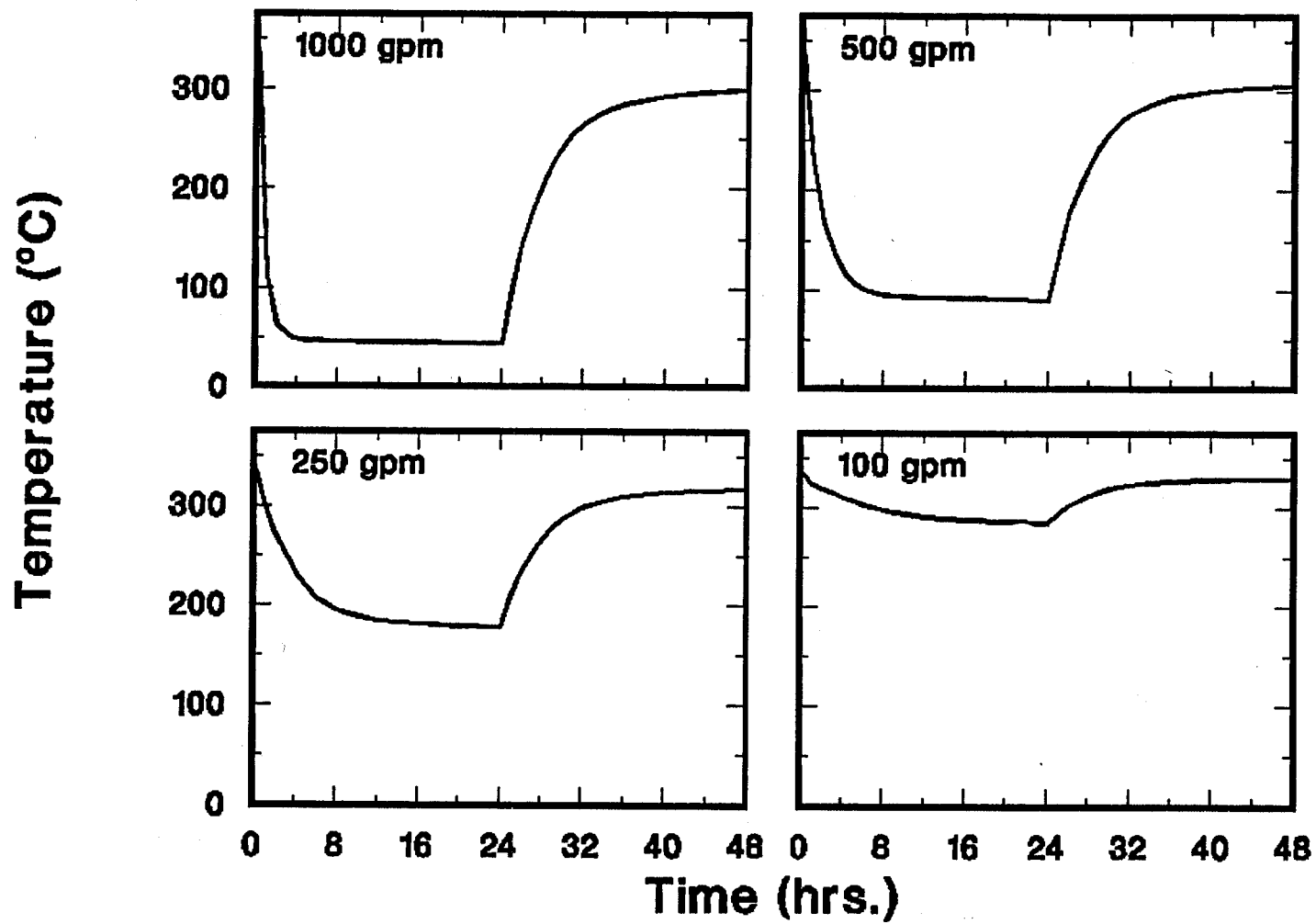


Figure 3-18. Bottom-hole temperatures as a function of time during circulation and following shut-in at four flow rates for the Salton Sea well model.

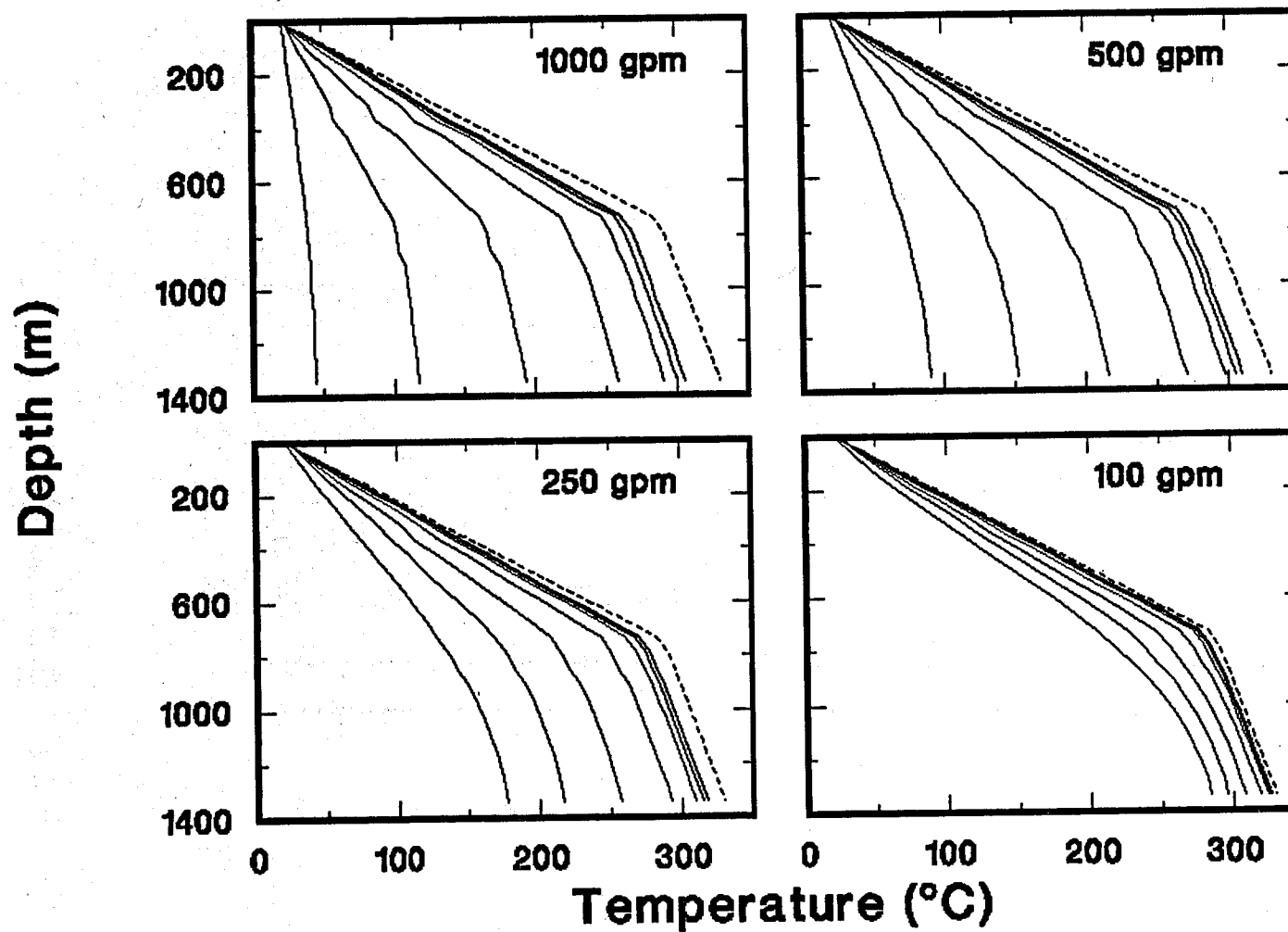


Figure 3-19. The downhole temperature profiles inside the tubing at times of 0, 2, 5, 10, 12, 16, and 24 hours following shut-in at four flow rates for the Salton Sea well model. The dashed line is the undisturbed temperature gradient.

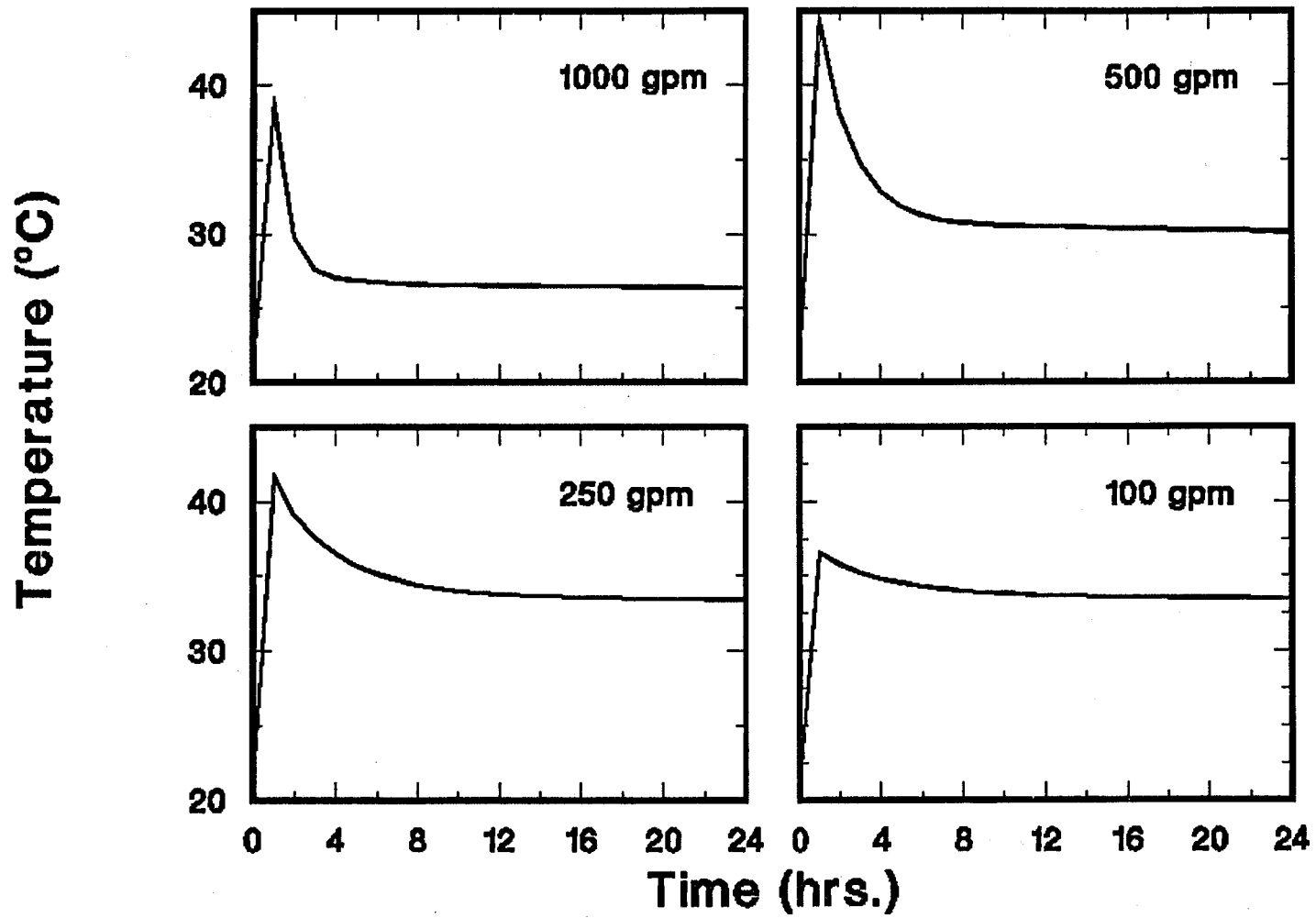


Figure 3-20. The return temperatures at the surface in the annulus at four flow rates for the Salton Sea well model.

Table 3-4. Salton Sea Geothermal Area. Shut-in temperatures at the bottom of the hole for three cases:

- A - Standard Wellbore
- B - Three Casing Strings
- C - Reduced Tubing Diameter

| Case | Flow Rate (gpm) | Shut-in Temperatures, °C, at |     |     |     |     |     |           |
|------|-----------------|------------------------------|-----|-----|-----|-----|-----|-----------|
|      |                 | 0                            | 1   | 2   | 5   | 10  | 16  | 24 (hrs.) |
| A    | 1000            | 44                           | 99  | 145 | 228 | 278 | 293 | 299       |
|      | 500             | 90                           | 137 | 176 | 246 | 288 | 301 | 306       |
|      | 250             | 178                          | 208 | 233 | 278 | 306 | 314 | 317       |
|      | 100             | 285                          | 294 | 302 | 316 | 326 | 328 | 329       |
| B    | 1000            | 47                           | 78  | 108 | 172 | 233 | 267 | 287       |
|      | 500             | 93                           | 121 | 145 | 199 | 250 | 279 | 296       |
|      | 250             | 177                          | 196 | 212 | 247 | 279 | 298 | 309       |
|      | 100             | 278                          | 285 | 291 | 302 | 313 | 319 | 323       |
| C    | 1000            | 28                           | 64  | 101 | 179 | 249 | 286 | 303       |
|      | 500             | 44                           | 80  | 114 | 188 | 255 | 288 | 304       |
|      | 250             | 93                           | 124 | 152 | 213 | 268 | 296 | 309       |
|      | 100             | 217                          | 232 | 245 | 274 | 301 | 314 | 321       |

### 3.2.2 MODIFIED WELLBORE CALCULATIONS AND RESULTS

Two changes were made to the standard wellbore to observe the effect on the downhole temperature calculations. These changes were: 1) the removal of the fourth casing (the 7-inch liner) so that only three casings were present in the wellbore; and 2) the reduction of the dimensions of the 5.5-inch tubing to one-half its previous value while keeping all four of the casing strings as in standard wellbore calculations. Both of these changes would be expected to have an effect on the heat transfer rate between the soil and the wellbore.

#### THREE CASING STRINGS

The wellbore was modified by removal of the 7-inch casing string. The bottom of the hole was open allowing direct interaction between the circulating fluid and the soil. The circulation and shut-in temperatures at the four flow rates are plotted as a function of time in Figure 3-21. The corresponding down-hole temperature profiles after shut-in are shown in Figure 3-22. And, finally, the midpoints of the warming curves for the three-casing case are compared to the standard wellbore case in Table 3-5.

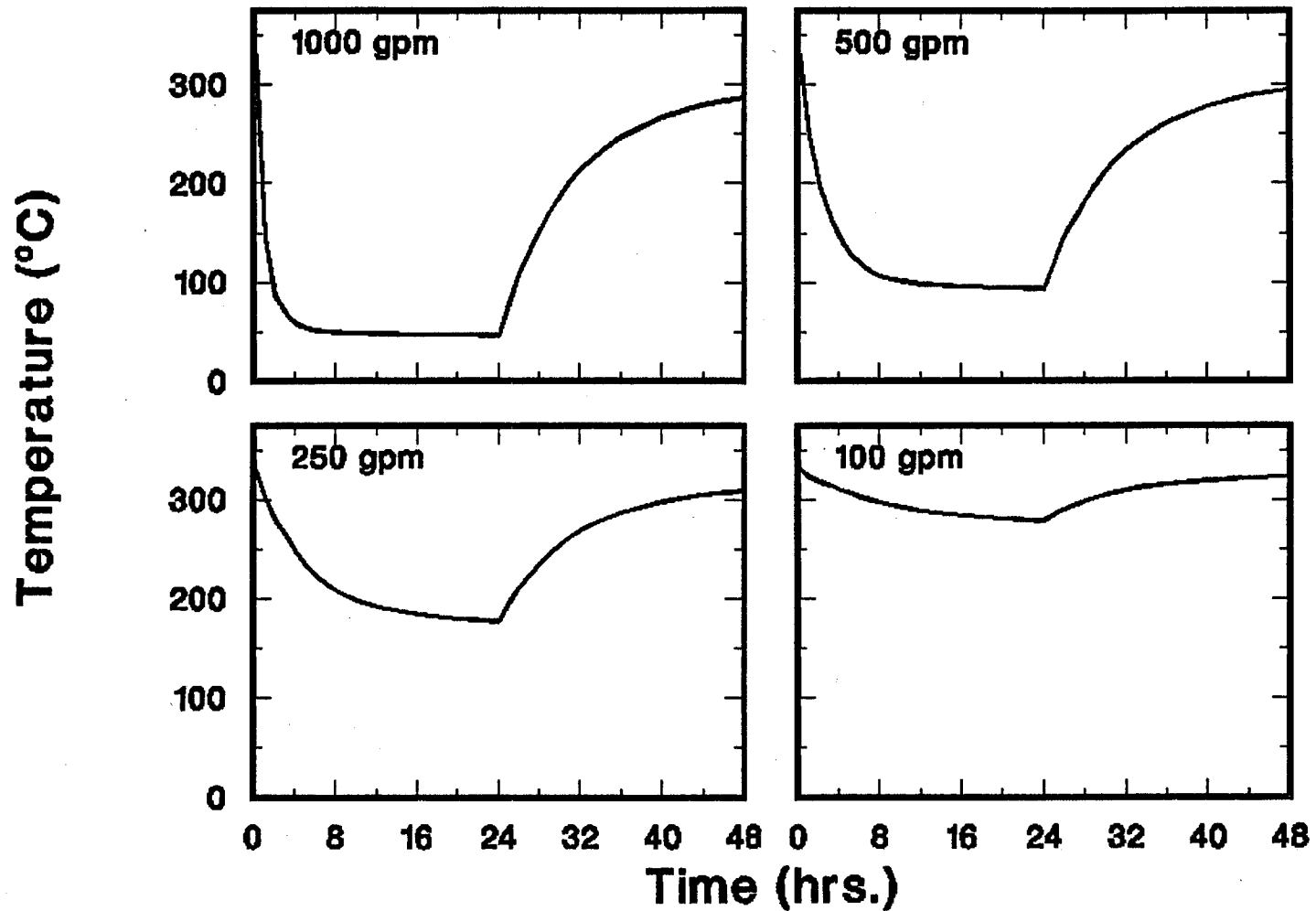


Figure 3-21. Bottom-hole temperatures as a function of time during circulation and following shut-in at four flow rates for the Salton Sea well model using three casings in the wellbore.

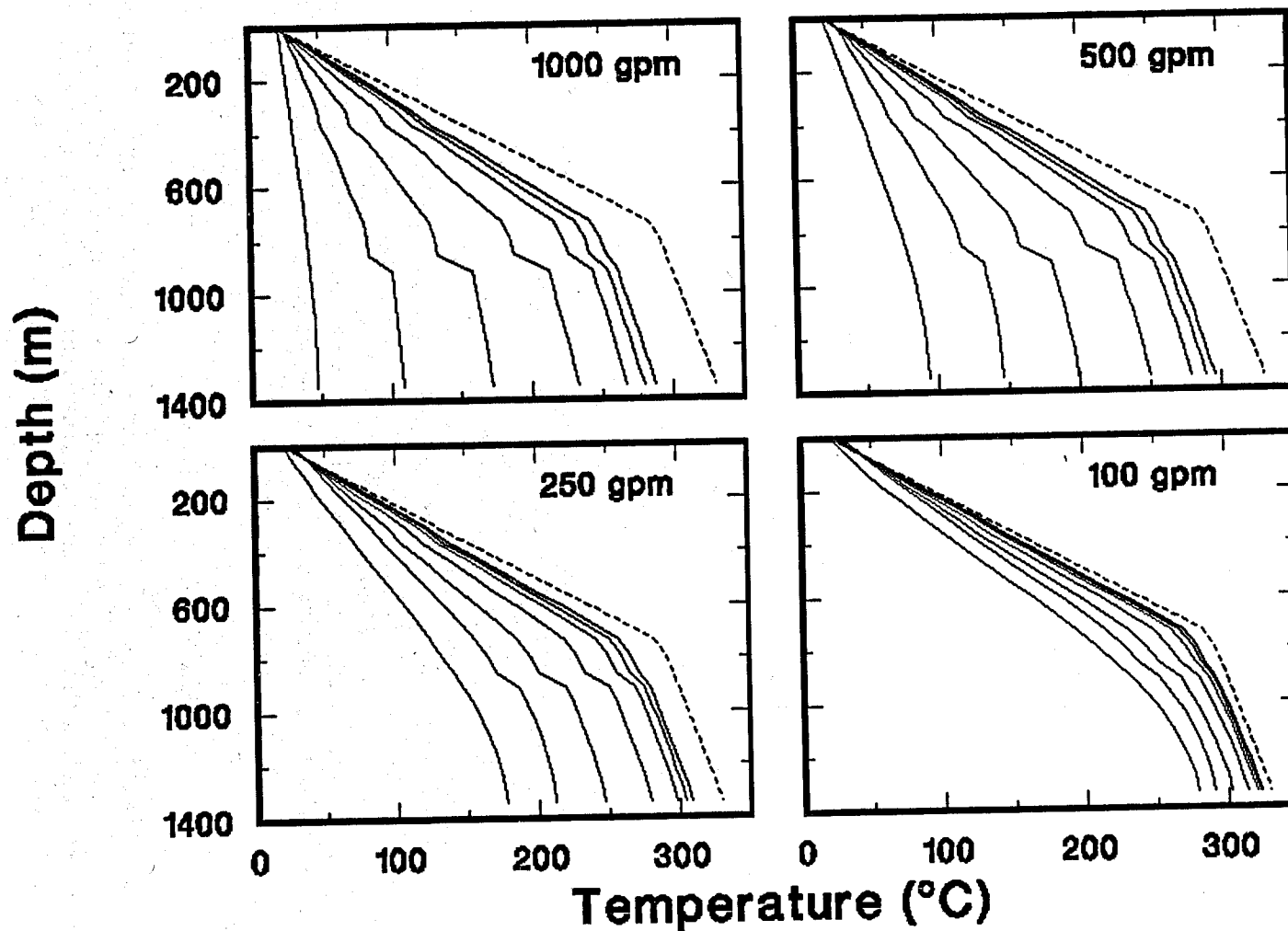


Figure 3-22. The downhole temperature profiles inside the tubing at times of 0, 2, 5, 10, 12, 16, and 24 hours following shut-in at four flow rates for the Salton Sea well model using three casings in the wellbore. The dashed line is the undisturbed temperature gradient.

Table 3-5. Comparison of the midpoints of the shut-in temperature curves for the Salton Sea geothermal area well model for three cases:

- A - Standard Wellbore
- B - Three Casing Strings
- C - Reduced Tubing Diameter

| Case | Flow Rate (gpm) | Mid-point temp. (°C) | Approx. time (hrs.) |
|------|-----------------|----------------------|---------------------|
| A    | 1000            | 172                  | 3.                  |
|      | 500             | 198                  | 3.                  |
|      | 250             | 248                  | 3.                  |
|      | 100             | 307                  | 3.5                 |
| B    | 1000            | 167                  | 5.                  |
|      | 500             | 194                  | 5.                  |
|      | 250             | 243                  | 5.                  |
|      | 100             | 301                  | 5.                  |
| C    | 1000            | 166                  | 4.5                 |
|      | 500             | 174                  | 4.5                 |
|      | 250             | 202                  | 4.5                 |
|      | 100             | 269                  | 4.5                 |

Comparing these figures to Figures 3-18 and 3-19 for the standard wellbore case and comparing the bottom-hole temperatures tabulated in Table 3-4 for the two cases, it is apparent that removal of the 7-inch casing has produced little or no effect on the minimum bottom-hole temperature after 1 day of circulation. However, the shapes of the cooling and warming curves are significantly different for the two cases. Table 3-5 shows that the mid-point temperatures of the curves for the three-casing and standard wellbore case are similar. However, the standard wellbore case is observed to warm significantly faster than the three-casing case. Note also that a pronounced cooling effect is observed above 914 m (3000 ft) at the higher flow rates.

#### REDUCED TUBING SIZE

The second modification made to the wellbore was reducing the diameter of the tubing to about one-half its value in the standard wellbore case. The calculations were made with all other features of the standard wellbore unchanged; specifically, the use of four casing strings was maintained.

The temperatures during circulation and following shut-in obtained from the calculations on this case are plotted in Figure 3-23. The corresponding downhole temperature profiles are shown in Figure 3-24. Comparing these figures with Figures 3-18 and 3-19 and the data tabulated in Tables 3-4 and 3-5, several observations can be made. Both the minimum bottom-hole temperatures during circulation and the shape of the cooling and warming curves are affected. The maximum temperatures reached after shut-in are not changed due to the reduced tubing diameter. Note that in contrast to the three-casing case, the mid-point temperatures, given in Table 3-5, are reduced for all but the 1000-gpm flow rate while the mid-point times are essentially unchanged compared to the three-casing case but longer than the standard case. The highest flow rate is not significantly affected by the change in tubing dimensions.

The downhole temperature profiles show a significant cooling effect when compared to the standard wellbore calculations. The cause of this cooling effect is quite complex. Figure 3-25 plots the temperatures after 1 day of circulation at 1220 m (4000 ft) for the first five radial grids extending roughly to 1.3 m (4.3 ft) into the soil formation from the wellbore centerline. Note that the soil in the immediate vicinity of the wellbore has cooled significantly for the reduced tubing diameter case. However, analysis of Eqn. 2-1 shows that the heat transfer coefficient,  $h$ , for the fluid/casing interface in the annulus is about three times larger in the standard wellbore case than in the reduced diameter case. On the basis of this, the standard wellbore case should be producing lower temperatures in the soil than the reduced diameter case. Since the volume flow rates for the two cases are identical, the velocities within the tubing and annulus must be different in the two cases. The fluid velocity in the tubing is about a factor of five larger for the reduced tubing diameter case. What this does is to get the fluid down the tubing faster in the smaller diameter tubing and, therefore, the fluid will be much cooler at the bottom of the hole than for the larger diameter tubing. The heat transferred the fluid to the soil (or the casing) is proportional not only to  $h$  but also to the temperature difference between the two. Hence, the fluid down the wellbore is cooler due to its higher velocity and is thus able to transfer more heat from the surrounding soil to the fluid. This effect becomes more important as the flow rate decreases as is shown in Figure 3-25.

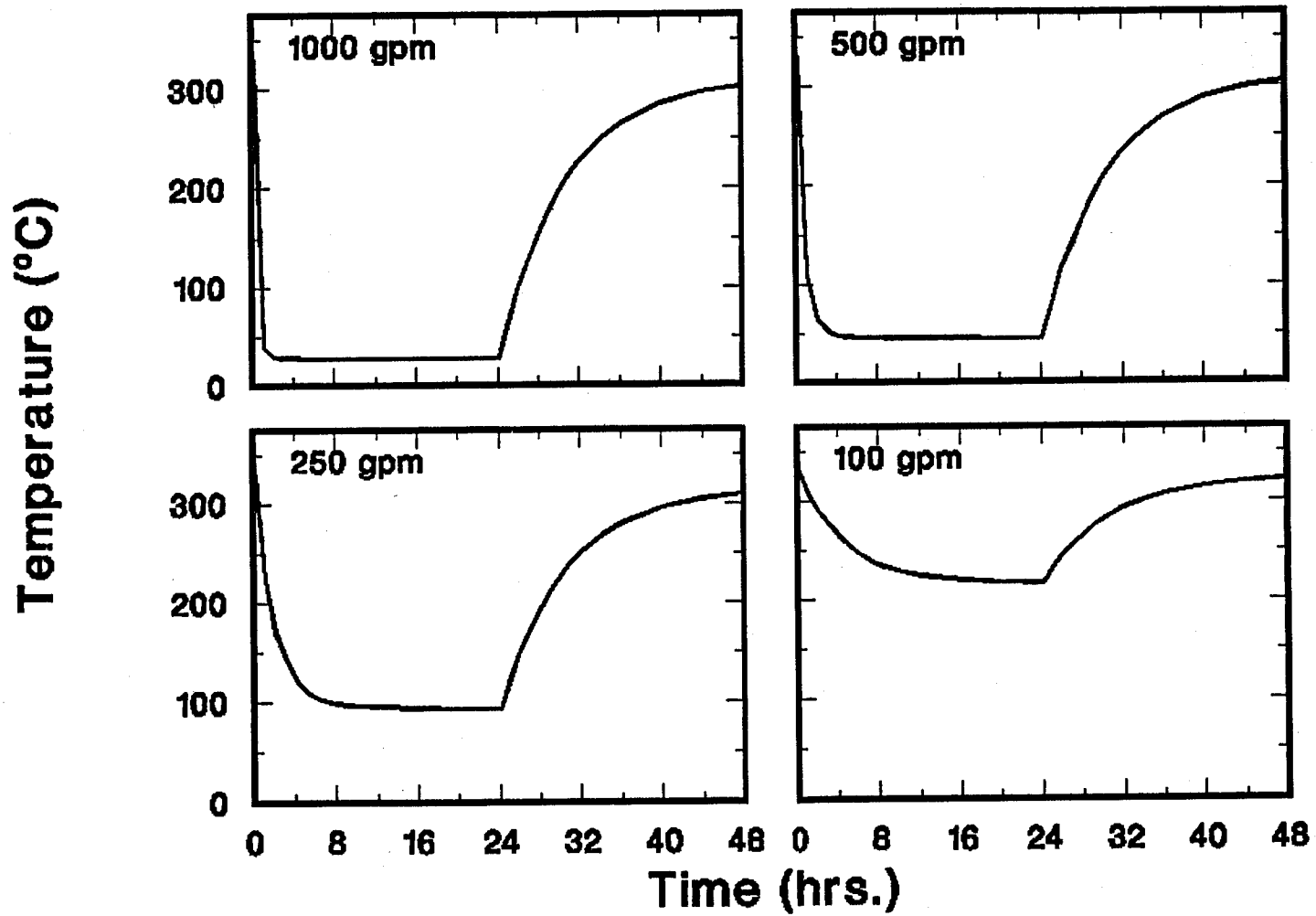


Figure 3-23. Bottom-hole temperatures as a function of time during circulation and following shut-in at four flow rates for the Salton Sea well model using a reduced tubing diameter in the wellbore.

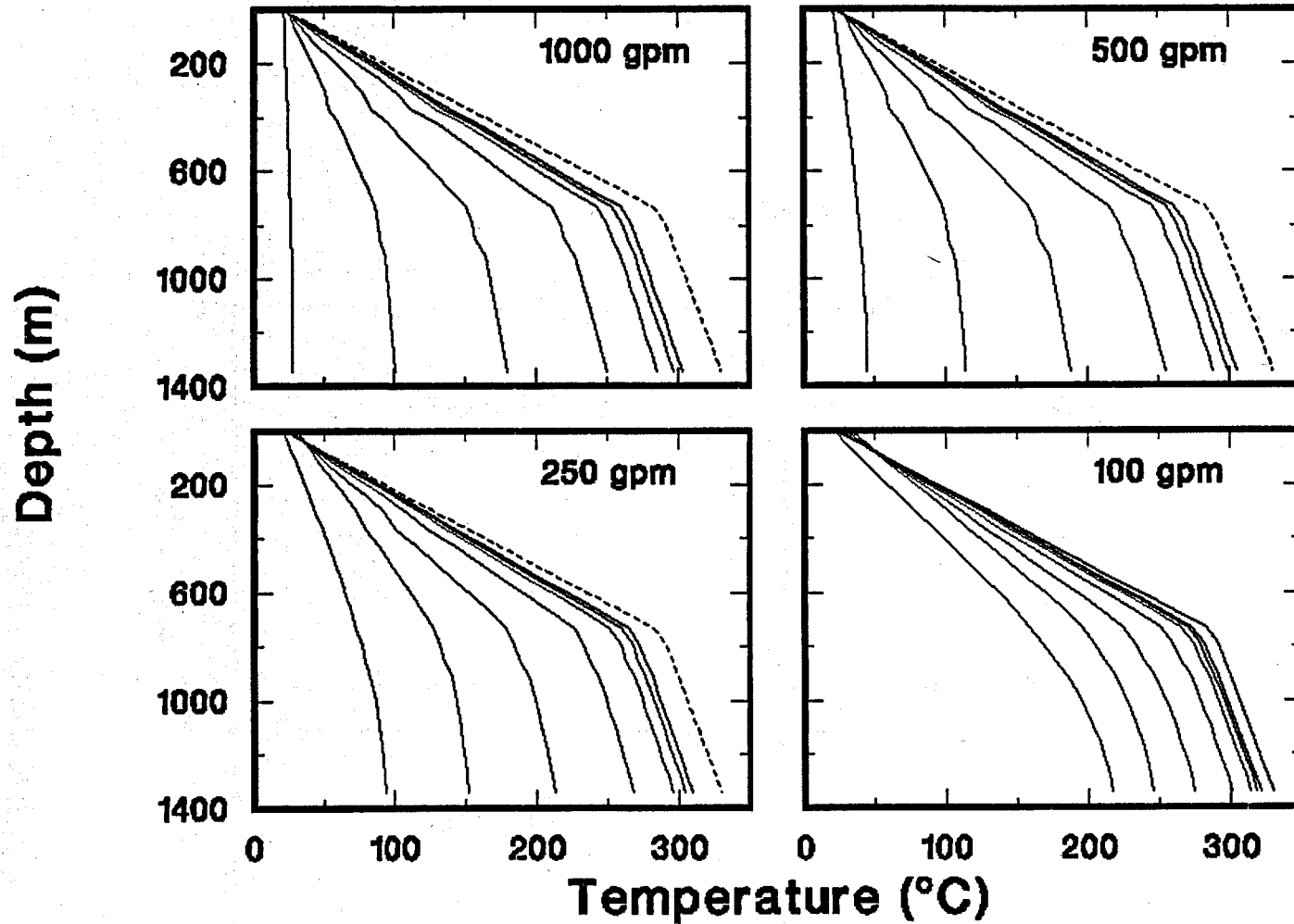


Figure 3-24. The downhole temperature profiles inside the tubing at times of 0, 2, 5, 10, 12, 16, and 24 hours following shut-in at four flow rates for the Salton Sea well model using a reduced tubing diameter in the wellbore. The dashed line is the undisturbed temperature gradient.

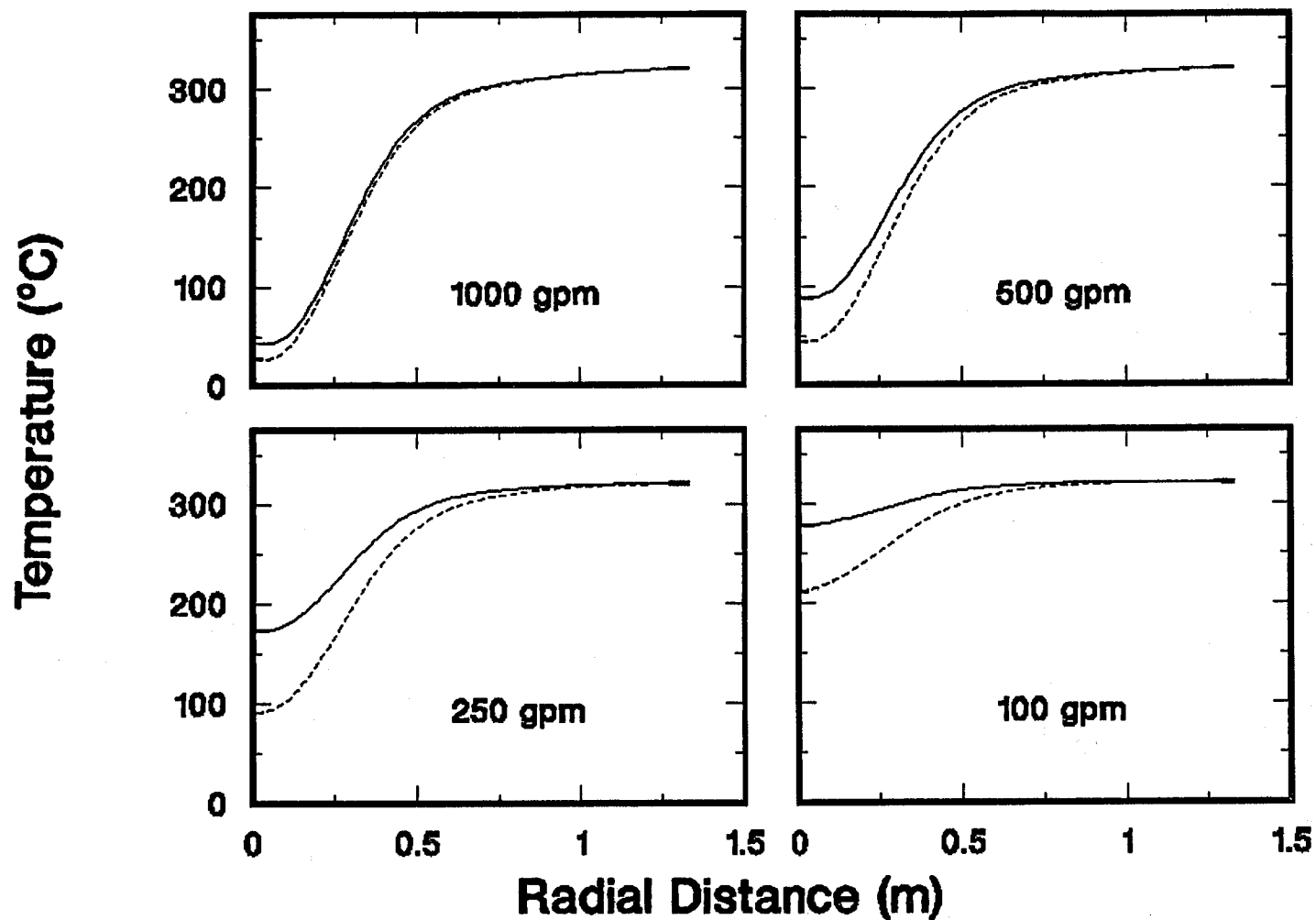


Figure 3-25. Comparison of the radial temperature profiles for the standard wellbore and reduced tubing diameter case at flow rates of 100, 250, 500, and 1000 gpm. Temperatures are plotted at a depth of 1220 m (4000 ft). The dashed line is the reduced tubing diameter case.

### 3.3 EAST MESA WELL MODEL

The standard wellbore description and geothermal profile for the East Mesa well model is illustrated in Figure 3-26. Total well depth was 2320 m (7600 ft). A 20-inch casing reached a depth of 30 m (100 ft) and was cemented to the surface. A 13-3/8-inch casing extended to 518 m (1700 ft) and was also cemented to the surface. A third casing of 9-5/8-inches reached a depth of 1680 m (5500 ft) and was cemented from the bottom of the casing up to a depth of 457 m (1500 ft). Finally, the fourth 7-inch casing extended to the bottom of the hole at 2320 m (7600 ft). 5.5-inch tubing was used in this simulation.

The undisturbed geothermal profile consisted of two linear temperature components [5]. The first linear profile extends from the surface (set nominally at 21°C (70°F) to a depth of 625 m (2050 ft) where the temperature was fixed at 152°C (305°F). The second temperature profile begins at this depth and extends to the bottom of the hole where the temperature was set at 204°C (400°F).

#### 3.3.1 STANDARD WELLBORE CALCULATIONS AND RESULTS

The soil thermal conductivity of the East Mesa KGRA is reported to be in the range of 0.75 to 1.02 Btu/ft hr °F [5]. For these calculations a value of 1.0 Btu/ft hr °F has been chosen. The temperatures obtained for water circulation and following shut-in are presented in Figure 3-27 for the four flow rates of 100, 250, 500, and 1000 gpm. The shut-in temperature profiles are shown in Figure 3-28 and the bottom-hole temperatures at several times after shut-in are given in Table 3-6.

Table 3-6. East Mesa Geothermal Area. Shut-in temperatures at the bottom of the hole.

| Flow Rate<br>(gpm) | Shut-in Temperatures, °C, at |     |     |     |     |     |           |
|--------------------|------------------------------|-----|-----|-----|-----|-----|-----------|
|                    | 0                            | 1   | 2   | 5   | 10  | 16  | 24 (hrs.) |
| 1000               | 59                           | 80  | 98  | 136 | 166 | 179 | 186       |
| 500                | 112                          | 126 | 137 | 161 | 180 | 188 | 193       |
| 250                | 166                          | 171 | 176 | 186 | 194 | 198 | 199       |
| 100                | 193                          | 194 | 196 | 198 | 201 | 202 | 203       |

### WELLBORE GEOMETRY AND GEOTHERMAL GRADIENT FOR THE EAST MESA KGRA

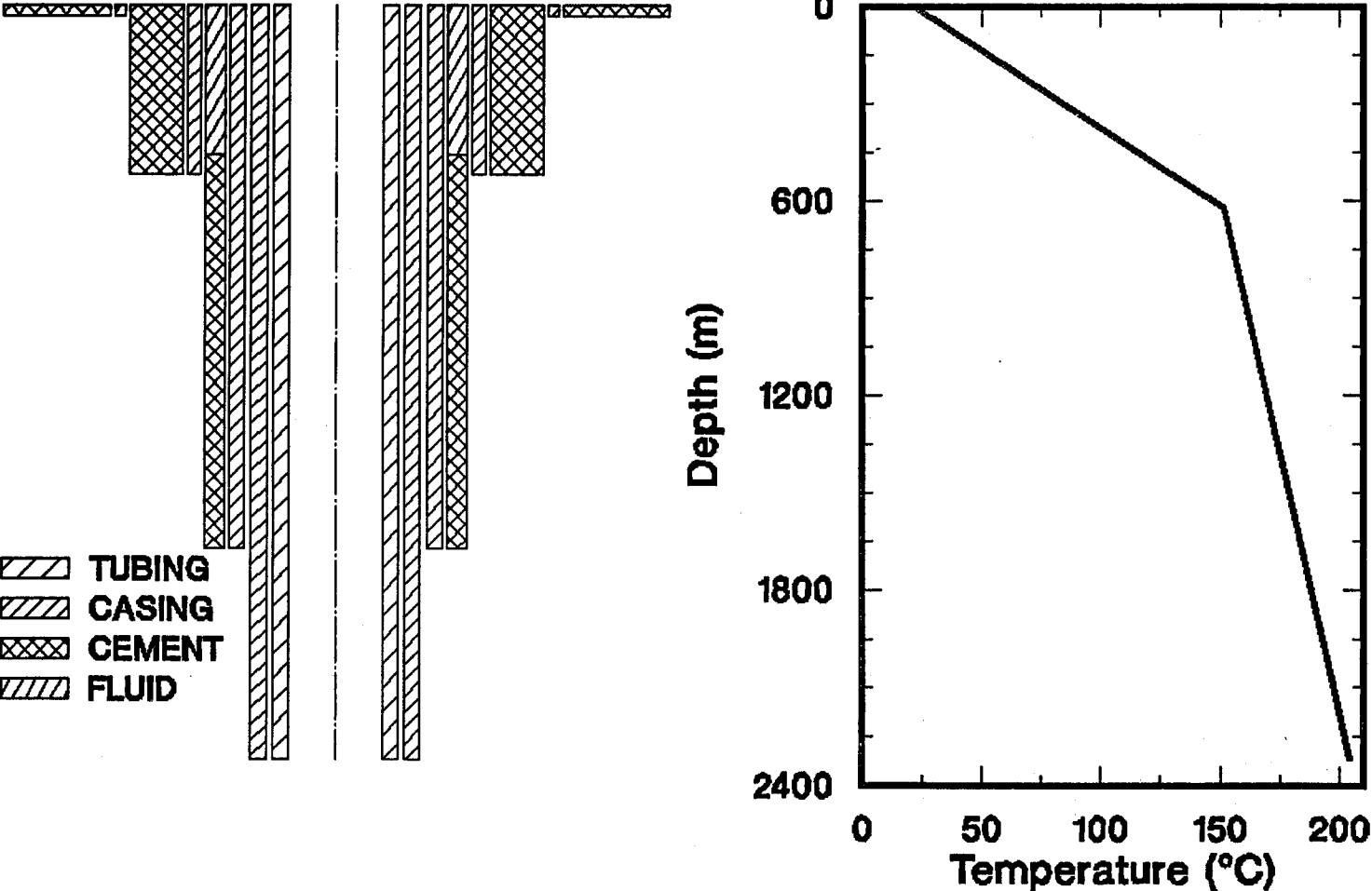


Figure 3-26. The wellbore geometry and undisturbed temperature gradient used in the East Mesa well model calculations.

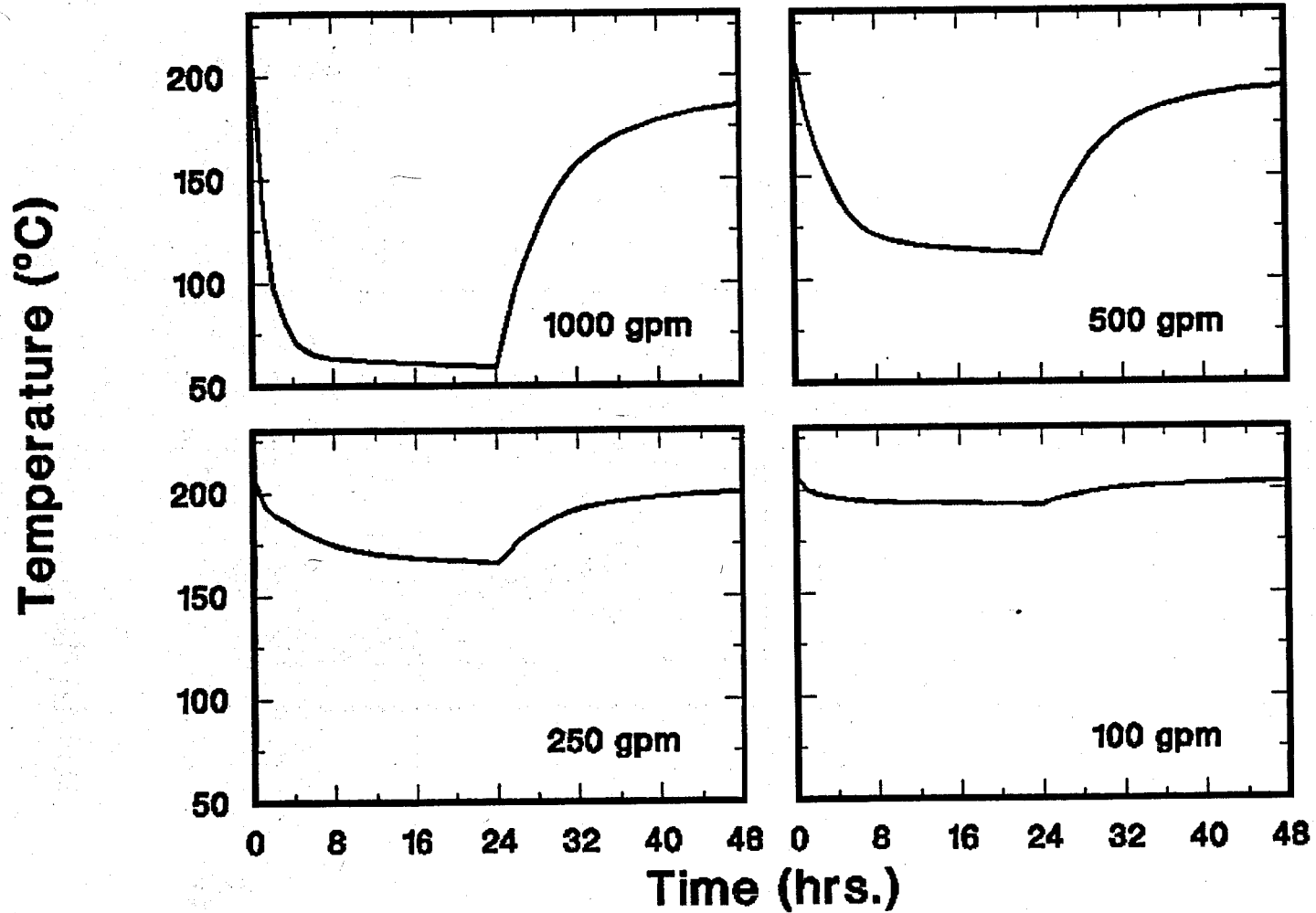


Figure 3-27. Bottom-hole temperatures as a function of time during circulation and following shut-in at four flow rates for the East Mesa well model.

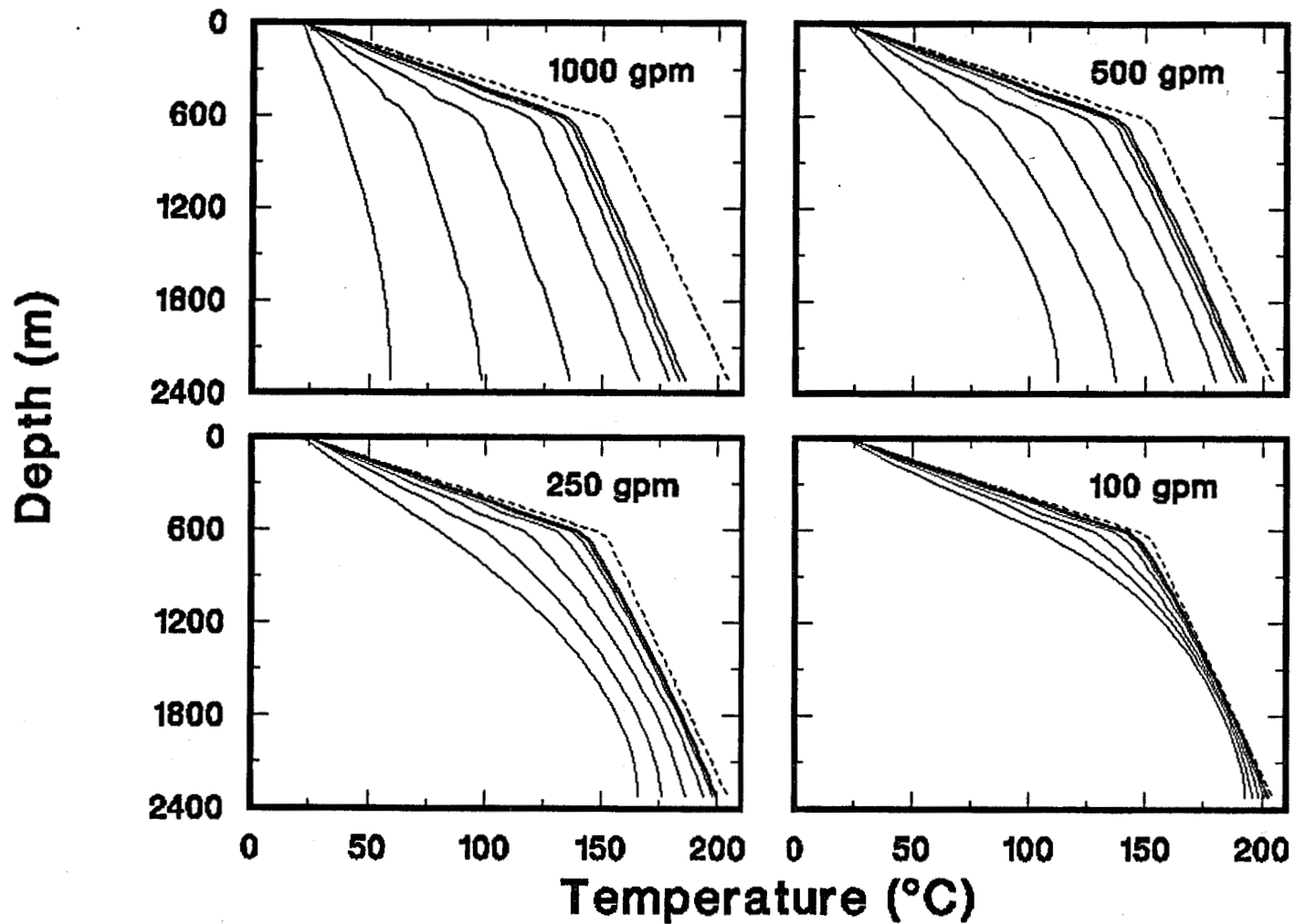


Figure 3-28. The downhole temperature profiles inside the tubing at times of 0, 2, 5, 10, 12, 16, and 24 hours following shut-in at four flow rates for the East Mesa well model. The dashed line is the undisturbed temperature gradient.

As in the previous well models, the flow rate of 100 gpm is ineffective in cooling the wellbore. Even though the maximum temperature is only 204°C (400°F), the bottom of the wellbore tends to be warmer than either the Baca or the Salton Sea standard wellbore at the flow rates of 500 and 1000 gpm but cooler than these at the lower flow rates of 100 and 250 gpm. At the higher flow rates the warmer temperatures are undoubtedly due to the greater depth of the well; the water is in contact with high temperatures a longer period of time and thus has a better opportunity to equilibrate at these higher temperatures. The relatively cooler temperatures at the lower flow rates is due to the lower bottom-hole temperature associated with this well model compared to either the Baca or the Salton Sea well model. Obviously, because of the lower bottom-hole temperatures the wellbore temperatures are not very hot, however, as Figure 3-27 clearly shows, the wellbore warms quite fast. At a flow rate of 1000 gpm, the temperature is near 100°C at 2 hours after shut-in and by 8 hours approaches 150°C.

### 3.4 DEEP SALTON SEA WELL MODEL

The standard wellbore description and geothermal profile for the Deep Salton Sea well model are illustrated in Figure 3-29. Total well depth was 5490 m (18,000 ft). A 24-inch casing reached a depth of 100 m (320 ft) and was cemented to the surface. A 16-inch casing extended to 975 m (3200 ft) and was also cemented to the surface. A third casing of 11-3/4 inches reached a depth of 2440 m (8000 ft) and was cemented from the bottom of the casing up to a depth of 975 m (3200 ft). Finally, the fourth 8-5/8-inch casing extended to 3660 m (12,000 ft). No casing was present in the hole from 3660 m to the bottom. 5.5-inch tubing was used in this simulation.

The undisturbed geothermal profile consisted of two linear temperature components. The first linear profile extends from the surface (set nominally at 21°C (70°F)) to a depth of 1600 m (5250 ft) where the temperature was fixed at 250°C (480°F) [5]. The second temperature profile begins at this depth and extends to the bottom of the hole where the temperature was set at 300°C (570°F).

#### 3.4.1 STANDARD WELLBORE CALCULATIONS AND RESULTS

As for the Salton Sea well model, the soil thermal conductivity used in the calculations was 1.0 Btu/ft hr°F. The temperatures obtained during water circulation and following shut-in are illustrated in Figure 3-30. The corresponding downhole temperature profiles at selected times after shut-in are shown in Figure 3-31. The bottom-hole temperatures after shut-in are tabulated in Table 3-7 below.

Table 3-7. Salton Sea Geothermal Area Deep Well. Shut-in temperatures at the bottom of the hole.

| Flow Rate<br>(gpm) | Shut-in Temperatures, °C, at |     |     |     |     |     |           |
|--------------------|------------------------------|-----|-----|-----|-----|-----|-----------|
|                    | 0                            | 1   | 2   | 5   | 10  | 16  | 24 (hrs.) |
| 1000               | 221                          | 232 | 241 | 262 | 278 | 286 | 290       |
| 500                | 278                          | 281 | 283 | 288 | 293 | 296 | 297       |
| 250                | 291                          | 291 | 292 | 294 | 297 | 297 | 298       |
| 100                | 294                          | 295 | 296 | 297 | 298 | 298 | 298       |

## WELLBORE GEOMETRY AND GEOTHERMAL GRADIENT FOR THE SALTON SEA KGRA DEEP WELL

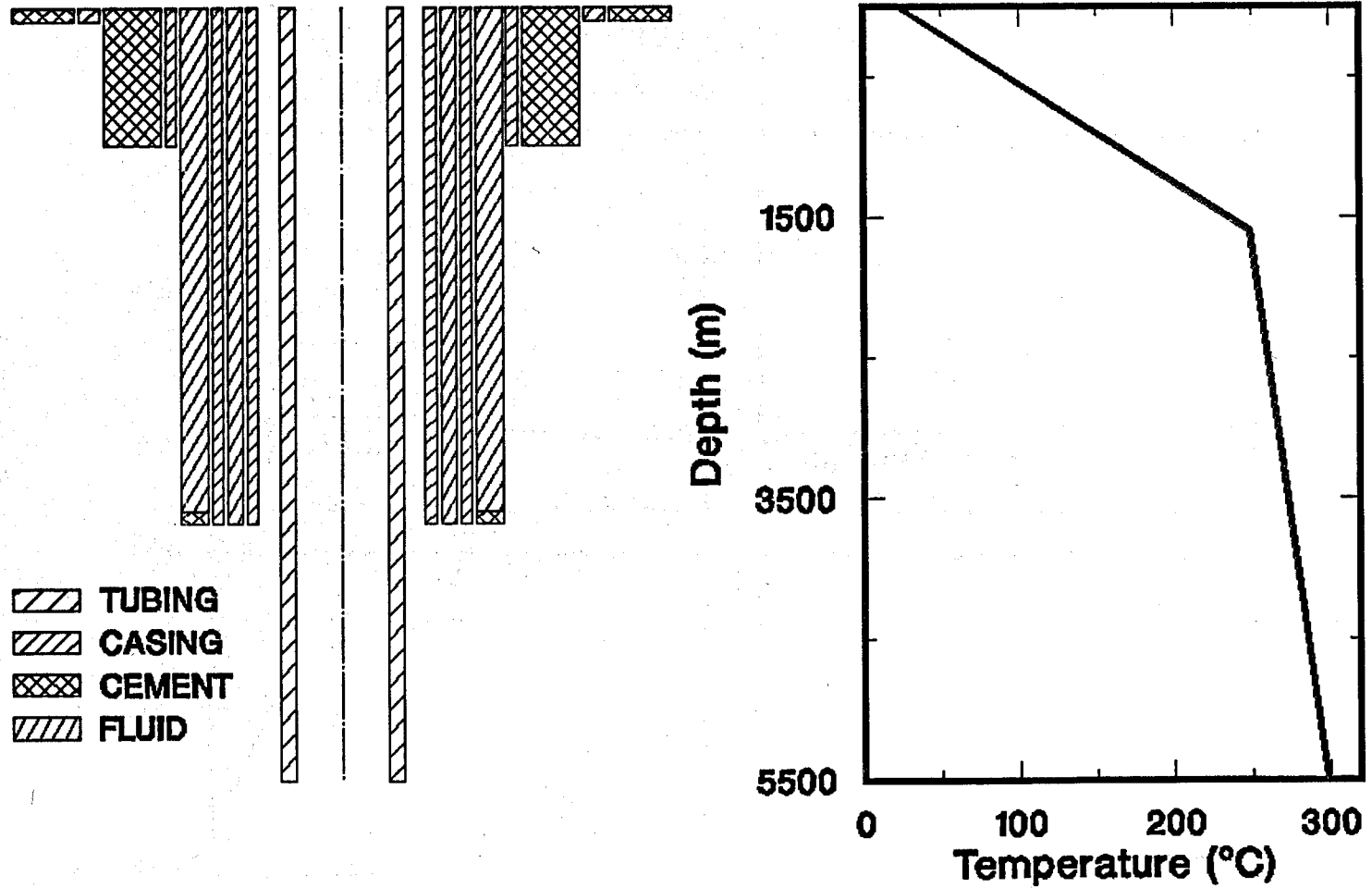


Figure 3-29. The wellbore geometry and undisturbed temperature gradient used in the Deep Salton Sea well model calculations.

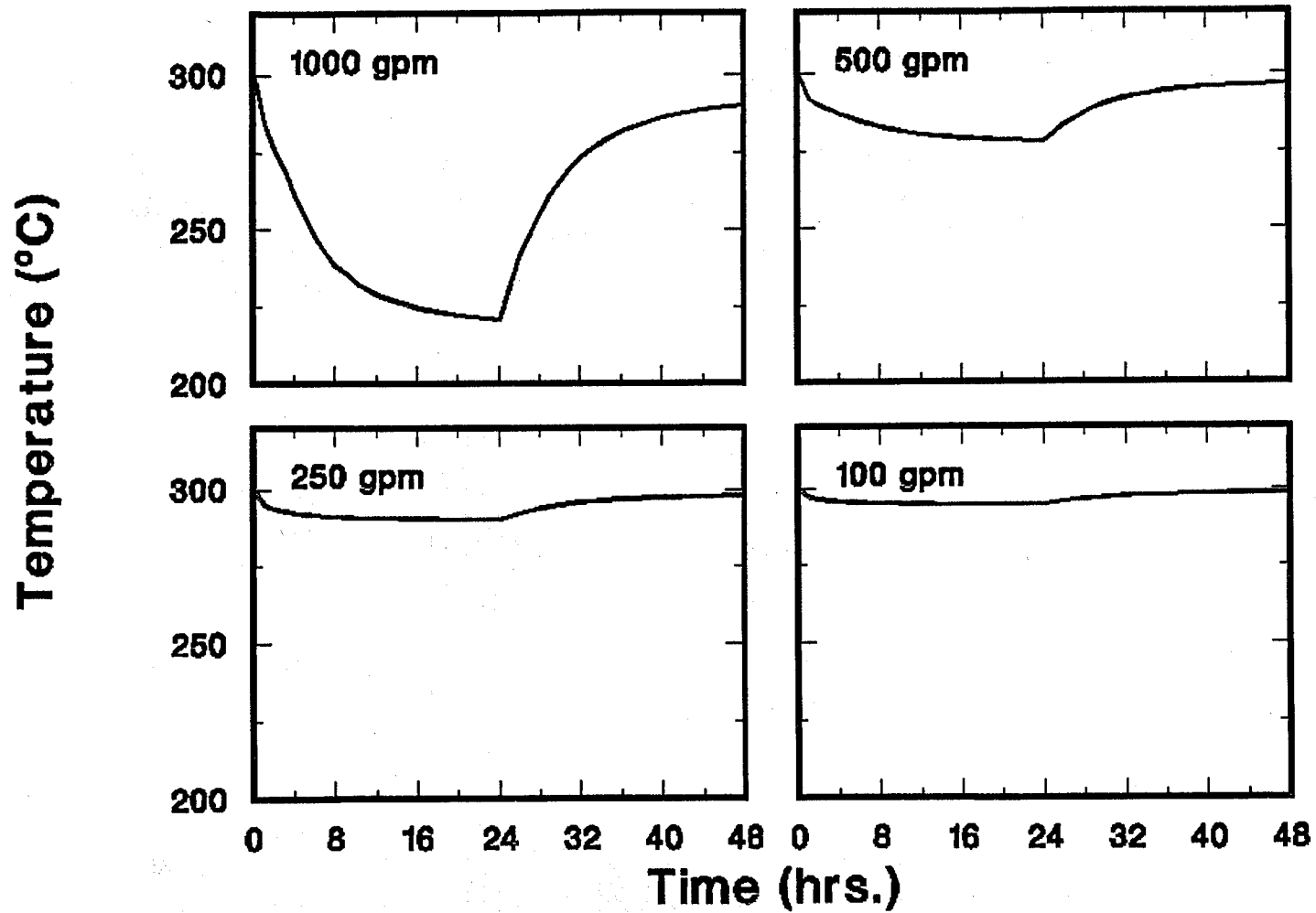


Figure 3-30. Bottom-hole temperatures as a function of time during circulation and following shut-in at four flow rates for the Deep Salton Sea well model.

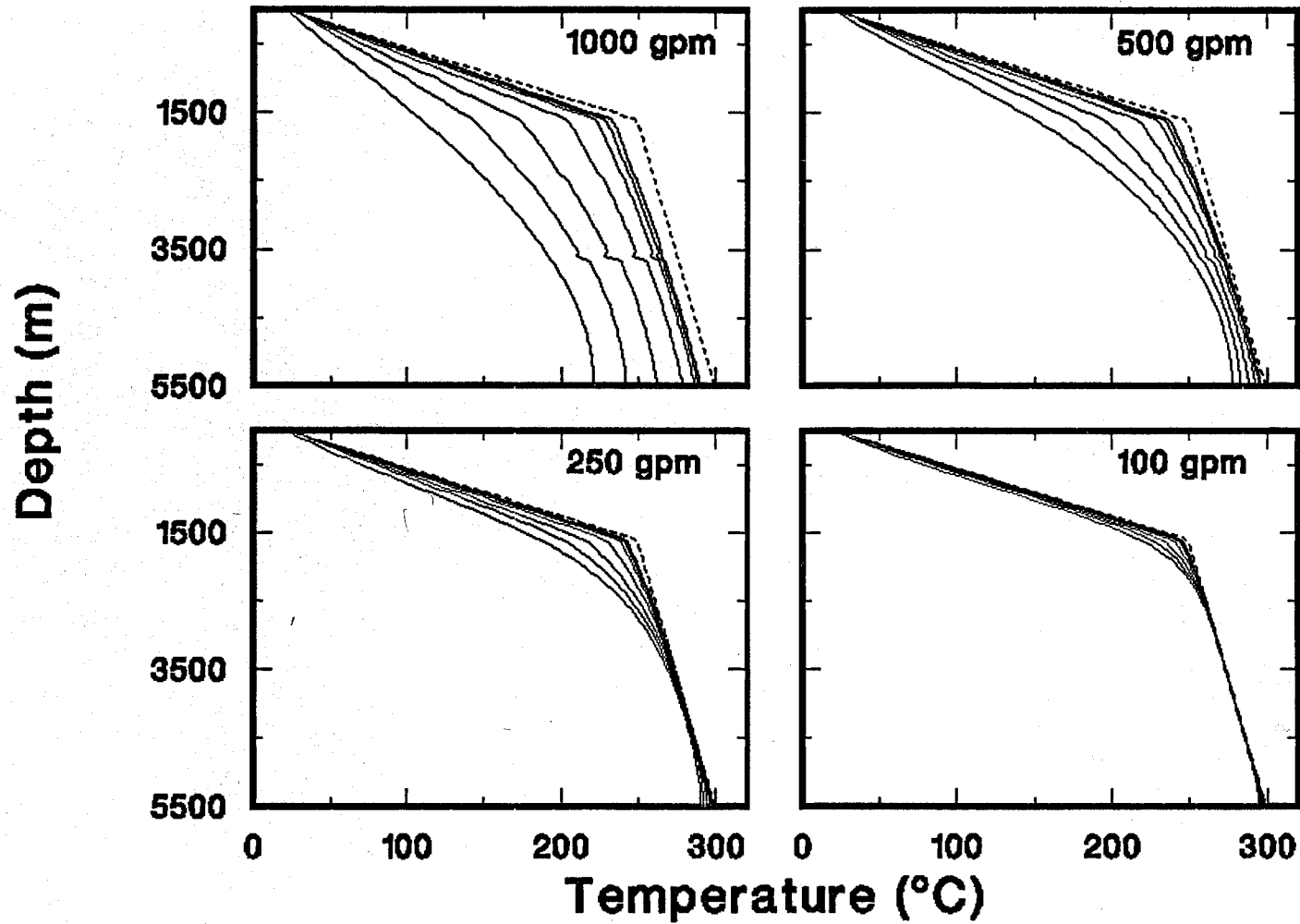


Figure 3-31. The downhole temperature profiles inside the tubing at times of 0, 2, 5, 10, 12, 16, and 24 hours following shut-in at four flow rates for the Deep Salton Sea well model. The dashed line is the undisturbed temperature gradient.

The temperatures obtained from these calculation are the hottest of all the well models studied. The flow rates of 100, 250, and 500 gpm, as evidenced by Figures 3-30 and 3-31, are very ineffective at cooling the down-hole environment. For example, the minimum temperature obtained for the 500-gpm flow rate was 278°C (532°F). The flow rate of 1000 gpm cools the bottom of the hole to 221°C (430°F), but the temperature quickly rises to over 250°C (482°F) at a time of only 4 hours after shut-in.

The steepness of the undisturbed temperature gradient has a substantial influence on the downhole cooling effect due to circulation. In the case shown here, the very steep initial gradient of near 0.16°C/m warms the fluid so that no cooling can take place below a depth of 1600 m where the gradient of 0.013°C/m is much less. This effect is most pronounced at the lowest flow rates where the longer residence times allow the fluid to warm to near the undisturbed soil temperature.

#### 4. SUMMARY AND CONCLUSIONS

Computer calculations of transient temperatures using the GEOTEMP2 computer code were made on four geothermal well models. The four well models studied were the Baca, Salton Sea, East Mesa, and a deep well in the Salton Sea area. Calculations were done using the wellbore models at flow rates of 100, 250, 500, and 1000 gpm for a one-day circulation time and a one-day shut-in period using water as the circulating fluid. In addition to this, calculations were done for the Baca and Salton Sea well model using either fluids other than water or modified wellbore geometries.

For the Baca well model, calculations using three values of the soil thermal conductivity,  $k$ , were made to observe the effect of  $k$  upon the downhole temperatures. It was found that lower values of  $k$  produced lower temperatures down the well during circulation and delayed the warming of the fluid after shut-in. Calculations were made with a water circulation time of 20 days. It was found that downhole temperatures were cooler both during circulation and following shut-in. The observed temperature differences between 1 and 20 days were greatest for the highest flow rate while soil thermal conductivity had a smaller effect. At a flow rate of 1000 gpm a temperature difference of 50°C was obtained 5 hours after shut-in and this difference was maintained through the rest of the one-day shut-in period.

In addition to water, two other circulating fluids were used in the Baca well model. A mud with a viscosity of 15 cp and the same density as water was found to produce lower downhole temperatures during circulation and cooler temperatures at a specified time after shut-in than in the comparable case using water. This difference was attributed to the reduced heat transfer rate of the mud with respect to water. Calculations were made using air as the circulating fluid at flow rates of 270 and 1090 scfm and a standpipe pressure of 1500 psi. The flow rates were chosen to correspond to the mass flow rates of the calculations made at water flow rates of 250 and 1000 gpm. The results of the calculations showed that air is completely ineffective as a cooling agent since bottom-hole temperatures were reduced less than 10°C from the undisturbed temperature at the highest flow rate.

For the Salton Sea well model, calculations were made at four water flow rates using  $k = 1.0$  Btu/ft hr °F. The results, as in the Baca well model, showed that the greater flow rates produced greater cooling. Bottom-hole temperatures tended to reach a value of one-half the difference between the undisturbed temperature and the minimum temperature achieved during circulation at a time of approximately 3 hours after shut-in.

Two modifications were made to the wellbore geometry of the Salton Sea well model. In the first modification, the fourth casing, which extended from the surface to the bottom of the hole, was removed. The calculations showed that the removal of the fourth casing did not alter the minimum bottom-hole temperatures obtained after one day of circulation. However, the shape of the warming curves was affected so that the bottom-hole temperatures reached a value of one-half of the difference between the undisturbed temperature and the temperature after one day of circulation at a

time of 5 hours, rather than 3 hours as in the original calculations, following shut-in. The second modification to the standard wellbore consisted of reducing the tubing diameter by a factor of about two. In these calculations the downhole temperatures were found to be significantly cooler than for either the standard wellbore or the three-casing case. Cooler bottom-hole temperatures were found but the time required to reach a temperature of one-half the difference between the undisturbed value and the minimum value was comparable to the standard wellbore and the three-casing case. The much cooler temperatures were attributed to the greater fluid velocity within the tubing due to the reduced tubing diameter. The cooling effect for this case was more pronounced at the lower flow rates than at the higher flow rates.

For the East Mesa well model, four flow rates were studied using a soil thermal conductivity value of 1.0 Btu/ft hr °F. The flow rate of 100 gpm was found to be ineffective in cooling the wellbore in agreement with the results of the previous well model calculations. The warming times following shut-in were comparable to results from the other well models though the temperatures tended to be cooler due to the lower maximum undisturbed temperature compared to the Baca or Salton Sea well model.

For the case of the deep Salton Sea well model, the downhole temperatures were found to be considerably higher than for the other well models. This result is due to the much greater depth, which allows the fluid more time to warm, and to the shape of the undisturbed geothermal gradient, which heats up the fluid at shallow depths thus reducing the potential cooling effect at greater depths.

Some conclusions about the cooling effect of circulation can be made as a result of this study. It is necessary to note that the calculations reported here treated heat transport only by conduction within the soil formation. In a real reservoir, other heat transport processes, such as convection of the fluid away from the wellbore or the presence of substantial fluid flow in the reservoir, can significantly modify the temperatures observed in the wellbore. The conclusions which can be drawn from this report are:

- o Higher flow rates produce the greatest cooling within the wellbore.
- o Low flow rates, on the order of 100 gpm or less, are particularly ineffective at cooling the wellbore.
- o Low soil thermal conductivity values produce lower wellbore temperatures due to the reduced rate of heat transfer.
- o High viscosity fluids, such as drilling muds, give lower wellbore temperatures because of the lower heat transfer rate.
- o Air or gas are ineffective as a cooling fluid.

- o The bottom-hole temperatures of deep wells tend to be much warmer than a shallow well during and after circulation, holding all conditions the same, due to the greater equilibration time of the fluid in the wellbore.
- o Downhole temperatures are not directly proportional to circulation time; the minimum downhole temperature is asymptotically approached as a function of time with short circulation times quickly approaching the limit.
- o The shape of the undisturbed temperature profile has a significant effect upon the downhole temperatures; high initial gradients tend to warm the fluid on the way down thus reducing the amount of cooling further down the hole.
- o An increased fluid velocity in the tubing, whether due to higher flow rates or a reduced tubing diameter, tends to decrease the downhole temperatures in the wellbore.

## REFERENCES

1. R. K. Traeger, S. G. Varnado, A. F. Venruso, V. L. Behr, and A. Ortega, "Drilling, Instrumentation, and Sampling Considerations for Geoscience Studies of Magma-Hydrothermal Regimes", SAND81-0800, Sandia National Laboratories, May 1981.
2. C. C. Carson, Y. T. Lin, and B. J. Livesay, "Representative Well Models for Eight Geothermal Resource Areas", SAND81-2202, Sandia National Laboratories, February 1983.
3. L. A. Mondy and L. E. Duda, "Advanced Wellbore Thermal Simulator - GEOTEMP2 - User Manual", SAND84-0857, Sandia National Laboratories.
4. T. D. Riney, J. W. Pritchett, and S. K. Garg, "Salton Sea Geothermal Reservoir Simulations", Geothermal Resources Council, TRANS., Vol. 2, July 1978, pp. 571-574.
5. T. D. Riney, J. W. Pritchett, and L. F. Rice, "Three-dimensional Model of East Mesa Hydrothermal System", Geothermal Resources Council, TRANS., Vol. 4, Sept. 1978, pp. 467-470.
6. Status Report of Geothermal Resource Investigations of the East Mesa Test Site, Imperial Valley, California, Status Report, Nov. 1974, U.S. Department of the Interior, Bureau of Reclamation.
7. R. F. Mitchell, "Advanced Wellbore Thermal Simulator - GEOTEMP2 - Research Report", SAND82-7003/1, Sandia National Laboratories, published February, 1982.
8. G. R. Wooley, "Wellbore and Soil Thermal Simulation for Geothermal Wells - Development of Computer Model and Acquisition of Field Temperature Data; Part I Report", SAND79-7119, Sandia National Laboratories, published March, 1980.
9. R. V. Guzowski, F. B. Nimick, and A. B. Muller, "Repository Site Definition in Basalt: Pasco Basin, Washington", NUREG/CR-2352, SAND81-2088, Sandia National Laboratories, March 1982.
10. D. W. Dareing, "Balanced Pressure Techniques Applied to Geothermal Drilling", SAND81-7130, Sandia National Laboratories, published August, 1981.
11. W. L. Wilkinson, Non-Newtonian Fluids, Pergamon Press, New York, 1960.
12. G. R. Wooley, "Wellbore and Soil Thermal Simulation for Geothermal Wells: Comparison of GEOTEMP predictions of Field Data and Evaluation of Flow Variables", SAND 79-7116, Sandia National Laboratories, published January, 1980.
13. J. Amand, W. H. Somerton, and E. Gomaa, "Predicting Thermal Conductivities of Formations from other known Properties", Soc. Pet. Eng. J., October 1973, pp. 267-273.

DISTRIBUTION:  
TID-4500-R-66-UC-66c (507)

Tom Anderson  
Venture Innovations  
P.O. Box 35845  
Houston, TX 77035

Dr. Khalid Aziz  
Stanford University  
Dept. of Petroleum Engineering  
Mitchell Building 360  
Stanford, CA 94305

Ed Bingman  
Shell Oil Company  
Two Shell Plaza  
P.O. Box 2099  
Houston, TX 77001

Larry Diamond  
Dyna-Drill  
P.O. Box C-19576  
Irvine, CA 92713

John E. Fontenot  
NL Petroleum Services  
P.O. Box 60087  
Houston, TX 77205

Dr. D. H. Freeston  
Geothermal Institute  
The University of Auckland  
Private Bag  
Auckland, New Zealand

Dr. Melvin Friedman  
Professor of Geology  
Center for Tectonophysics  
and Dept. of Geology  
Texas A&M University  
College Station, TX 77843

Nancy Jensen  
Union Oil Co.  
1410 Guerneville Rd.  
Santa Rosa, CA 95401

Paul Kasameyer  
Lawrence Livermore National Laboratory  
P.O. Box 808  
Livermore, CA 94550

James W. Langford  
Security Division  
Dresser Industries, Inc.  
P.O. Box 24647  
Dallas, TX 75224

Jill Lefforge  
Hughes Tool Division  
P.O. Box 2539  
Houston, TX 77001

B. J. Livesay  
129 Liverpool  
Cardiff, CA 92007

Harvey E. Mallory  
P.O. Box 54696  
Tulsa, OK 74155

Ed Martin  
Superior Oil  
Eastern Division  
P.O. Box 51108 OCS  
Lafayette, Louisiana 70505

Dr. Robert W. Nicholson  
Well Production Testing, Inc.  
P.O. Box 69  
Carlsbad, CA 92008

Gene Polk  
NL Baroid  
6400 Uptown Blvd. N.E., 365W  
Albuquerque, NM 87110

Del E. Pyle  
Union Geothermal Division  
Union Oil Co. of California  
Union Oil Center  
Los Angeles, CA 90017  
Attn: Deepak Kenkeremath

John C. Rowley  
Los Alamos National Labs  
Mail Stop 570  
Los Alamos, NM 87545

Dwight Smith  
Halliburton  
Drawer 1431  
Duncan, OK 73533

Tom Turner  
Phillips Petroleum Company  
Geothermal Operations  
655 East 4500 South  
Salt Lake City, UT 84107

Tom Warren  
Amoco Production Company  
Research Center  
P.O. Box 591  
Tulsa, OK 74102

U.S. Department of Energy (3)  
Geothermal Hydropower  
Technologies Division  
Forrestal Bldg., CE 324  
1000 Independence Ave. S.W.  
Washington, D.C. 20585  
Attn: J. Bresee  
R. Toms  
D. Allen

W. P. Grace, DOE/AL  
Nuclear & Geosciences Division

1512 L. A. Mondy  
3141 L. J. Erickson (5)  
3151 W. L. Garner (3)  
6000 E. H. Beckner  
6200 V. L. Dugan  
6240 R. K. Traeger  
6240A P. C. Lysne  
6241 J. R. Kelsey (20)  
6241 L. E. Duda (10)  
6242 J. C. Dunn  
6248 W. B. Gauster  
6250 B. W. Marshall  
8214 M. A. Pound